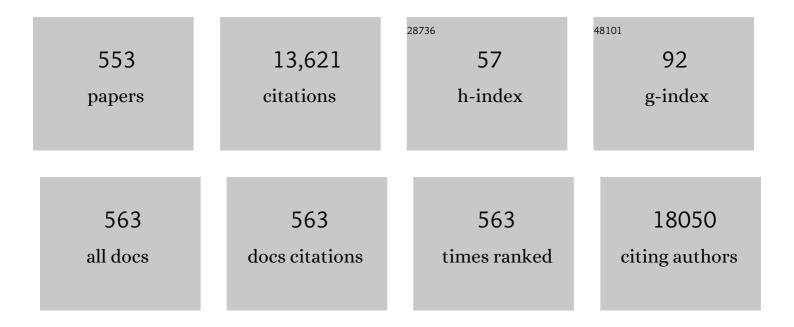
List of Publications by Year in descending order

Source: https://exaly.com/author-pdf/6896406/publications.pdf Version: 2024-02-01



ΖΟΙΤΑ:Ν ΚΑ3ΝΥΛ

#	Article	IF	CITATIONS
1	Photocatalytic CO2 Reduction. Green Chemistry and Sustainable Technology, 2022, , 605-646.	0.4	2
2	Nature of the Pt-Cobalt-Oxide surface interaction and its role in the CO2 Methanation. Applied Surface Science, 2022, 571, 151326.	3.1	23
3	Morphological aspects determine the catalytic activity of porous hydrocalumites: the role of the sacrificial templates. Materials Today Chemistry, 2022, 23, 100682.	1.7	6
4	Optimalization of ceramic-based noble metal-free catalysts for CO oxidation reactions. Reaction Kinetics, Mechanisms and Catalysis, 2022, 135, 575-587.	0.8	2
5	EDTA analogues – unconventional inhibitors of gypsum precipitation. Journal of Molecular Structure, 2022, 1256, 132491.	1.8	3
6	Pharmaceutical Development and Design of Thermosensitive Liposomes Based on the QbD Approach. Molecules, 2022, 27, 1536.	1.7	3
7	Effect of Excess B in Ni ₂ P-Coated Boron Nitride on the Photocatalytic Hydrogen Evolution from Water Splitting. ACS Applied Energy Materials, 2022, 5, 3578-3586.	2.5	17
8	Mechanochemical preparation of NiCuSn nanoparticles and composites in presence of cetyltrimethylammonium bromide (CTAB) and the catalytic application of the products in homocoupling and hydration of terminal alkynes. Journal of Molecular Structure, 2022, 1262, 132948.	1.8	2
9	Efficient charge separation and improved photocatalytic activity in Type-II & Type-III heterojunction based multiple interfaces in BiOCl0.5Br0.5-Q: DFT and Experimental Insight. Chemosphere, 2022, 297, 134122.	4.2	6
10	Exfoliation of black phosphorus in isopropanol-water cosolvents. Journal of Molecular Structure, 2022, 1260, 132862.	1.8	2
11	Preparation and characterization of MnIn-layered double hydroxides (LDHs), extension of the synthesis to fabricate MnM(III)-LDHs (MÂ=ÂAl, Sc, Cr, Fe, Ga), and the comparison of their photocatalytic and catalytic activities in the oxidation of hydroquinone. Journal of Molecular Structure, 2022, 1261, 132966.	1.8	4
12	Niacin and niacin-pillared layered double hydroxides—Novel organocatalysts based on pyridine. Journal of Molecular Structure, 2022, 1261, 132868.	1.8	2
13	Microscopic and structural study on the formation of mechanochemical synthesized BaTiO3 and ZnTiO3 perovskites. Resolution and Discovery, 2022, , .	0.9	Ο
14	Dependence of Photocatalytic Activity on the Morphology of Strontium Titanates. Catalysts, 2022, 12, 523.	1.6	7
15	Investigation of the adsorption properties of cyclic C6 molecules on h-BN/Rh(111) surface, efforts to cover the boron nitride nanomesh by graphene. Surfaces and Interfaces, 2022, , 102034.	1.5	2
16	Preparation of TiO2–MoO3 composite nanofibers by water-based electrospinning process and their application in photocatalysis. Materials Science in Semiconductor Processing, 2022, 147, 106699.	1.9	12
17	Mechanochemically induced solid-state CO2 capture during the synthesis of SnO2 nanoparticles. Journal of Physics and Chemistry of Solids, 2022, 167, 110775.	1.9	1
18	A round dance of acetaldehyde molecular ensembles on Rh(111) surface; formation and decomposition of various paraldehyde conformers. Journal of Molecular Structure, 2022, , 133311.	1.8	0

#	Article	IF	CITATIONS
19	Epigallocatechine-3-gallate Inhibits the Adipogenesis of Human Mesenchymal Stem Cells via the Regulation of Protein Phosphatase-2A and Myosin Phosphatase. Cells, 2022, 11, 1704.	1.8	2
20	Palladium Decorated N-Doped Carbon Foam as a Highly Active and Selective Catalyst for Nitrobenzene Hydrogenation. International Journal of Molecular Sciences, 2022, 23, 6423.	1.8	6
21	Interfacial charge separation of nickel phosphide anchored on anatase-hematite heterojunction for stimulating visible light driven hydrogen generation. International Journal of Hydrogen Energy, 2022, 47, 23593-23607.	3.8	8
22	Conversion Study on the Formation of Mechanochemically Synthesized BaTiO3. Chemistry, 2022, 4, 592-602.	0.9	1
23	Interfacial Ni active sites strike solid solutional counterpart in CO2 hydrogenation. Environmental Technology and Innovation, 2022, 27, 102747.	3.0	9
24	Thermal Conductivity Enhancement of Atomic Layer Deposition Surface-Modified Carbon Nanosphere and Carbon Nanopowder Nanofluids. Nanomaterials, 2022, 12, 2226.	1.9	3
25	Turning CO2 to CH4 and CO over CeO2 and MCF-17 supported Pt, Ru and Rh nanoclusters – Influence of nanostructure morphology, supporting materials and operating conditions. Fuel, 2022, 326, 124994.	3.4	6
26	Mechanochemical synthesis of the NiSn, CuSn bimetallic and NiCuSn trimetallic nanocomposites using various types of additives. Journal of Solid State Chemistry, 2021, 293, 121756.	1.4	3
27	A colloid chemistry route for the preparation of hierarchically ordered mesoporous layered double hydroxides using surfactants as sacrificial templates. Journal of Colloid and Interface Science, 2021, 581, 928-938.	5.0	26
28	Nitric oxide signalling in plant nanobiology: current status and perspectives. Journal of Experimental Botany, 2021, 72, 928-940.	2.4	13
29	Long-term effect of graphene oxide on the aerobic granular sludge wastewater treatment process. Journal of Environmental Chemical Engineering, 2021, 9, 104853.	3.3	12
30	Synthesis of iron oxide nanoparticles for DNA purification. Journal of Dispersion Science and Technology, 2021, 42, 693-700.	1.3	12
31	Exploiting a silver–bismuth hybrid material as heterogeneous noble metal catalyst for decarboxylations and decarboxylative deuterations of carboxylic acids under batch and continuous flow conditions. Green Chemistry, 2021, 23, 4685-4696.	4.6	7
32	Optimization of the functionalization method of titanate nanotubes in order to use them as drug delivery systems. , 2021, , .		0
33	Metallic Nanoparticles in Heterogeneous Catalysis. Catalysis Letters, 2021, 151, 2153.	1.4	50
34	Binder-Free Construction of a Methanol Tolerant Pt/TiO2/Carbon Paper Anode by Atomic Layer Deposition. Catalysts, 2021, 11, 154.	1.6	3
35	Preparation of TiO2/WO3/C/N Composite Nanofibers by Electrospinning Using Precursors Soluble in Water and Their Photocatalytic Activity in Visible Light. Nanomaterials, 2021, 11, 351.	1.9	4
36	Green Silver and Gold Nanoparticles: Biological Synthesis Approaches and Potentials for Biomedical Applications. Molecules, 2021, 26, 844.	1.7	142

#	Article	IF	CITATIONS
37	Specific Ion Effects on Aggregation and Charging Properties of Boron Nitride Nanospheres. Langmuir, 2021, 37, 2466-2475.	1.6	17
38	Complexity of a Co ₃ O ₄ System under Ambient-Pressure CO ₂ Methanation: Influence of Bulk and Surface Properties on the Catalytic Performance. Journal of Physical Chemistry C, 2021, 125, 7130-7141.	1.5	43
39	Composites of ion-in-conjugation polysquaraine and SWCNTs for the detection of H ₂ S and NH ₃ at ppb concentrations. Nanotechnology, 2021, 32, 185502.	1.3	7
40	Raman Spectral Signatures of Serum-Derived Extracellular Vesicle-Enriched Isolates May Support the Diagnosis of CNS Tumors. Cancers, 2021, 13, 1407.	1.7	10
41	Surface Engineering of CeO2 Catalysts: Differences Between Solid Solution Based and Interfacially Designed Ce1â`'xMxO2 and MO/CeO2 (M = Zn, Mn) in CO2 Hydrogenation Reaction. Catalysis Letters, 2 151, 3477-3491.	20241,	22
42	The dissolution kinetics of raw and mechanochemically treated kaolinites in industrial spent liquor – The effect of the physico-chemical properties of the solids. Applied Clay Science, 2021, 203, 105994.	2.6	6
43	Quality-by-Design-Based Development of n-Propyl-Gallate-Loaded Hyaluronic-Acid-Coated Liposomes for Intranasal Administration. Molecules, 2021, 26, 1429.	1.7	16
44	Oxidation of Cysteinate Anions Immobilized in the Interlamellar Space of CaAl-Layered Double Hydroxide. Materials, 2021, 14, 1202.	1.3	1
45	Stability of Boron Nitride Nanosphere Dispersions in the Presence of Polyelectrolytes. Langmuir, 2021, 37, 5399-5407.	1.6	2
46	Are Smaller Nanoparticles Always Better? Understanding the Biological Effect of Size-Dependent Silver Nanoparticle Aggregation Under Biorelevant Conditions. International Journal of Nanomedicine, 2021, Volume 16, 3021-3040.	3.3	62
47	Nesting Well-Defined Pt Nanoparticles within a Hierarchically Porous Polymer as a Heterogeneous Suzuki–Miyaura Catalyst. ACS Applied Nano Materials, 2021, 4, 4070-4076.	2.4	7
48	Evaluation of the permeability and in vitro cytotoxicity of functionalized titanate nanotubes on Caco-2 cell line. Acta Pharmaceutica Hungarica, 2021, 91, 31-39.	0.2	2
49	Damage-tolerant 3D-printed ceramics via conformal coating. Science Advances, 2021, 7, .	4.7	32
50	An Updated Risk Assessment as Part of the QbD-Based Liposome Design and Development. Pharmaceutics, 2021, 13, 1071.	2.0	11
51	Role of active metals Cu, Co, and Ni on ceria towards CO2 thermo-catalytic hydrogenation. Reaction Kinetics, Mechanisms and Catalysis, 2021, 133, 699-711.	0.8	2
52	Development of a Hydrophobicity-Controlled Delivery System Containing Levodopa Methyl Ester Hydrochloride Loaded into a Mesoporous Silica. Pharmaceutics, 2021, 13, 1039.	2.0	3
53	Microcystin-LR, a cyanobacterial toxin affects root development by changing levels of PIN proteins and auxin response in Arabidopsis roots. Chemosphere, 2021, 276, 130183.	4.2	6
54	Removing low levels of Cd(II) and Pb(II) by adsorption on two types of oxidized multiwalled carbon nanotubes. Journal of Environmental Chemical Engineering, 2021, 9, 105402.	3.3	36

#	Article	IF	CITATIONS
55	Manipulating the crystallization kinetics and morphology of gypsum, CaSO4·2H2O via addition of citrate at high levels of supersaturation and the effect of high salinity. Polyhedron, 2021, 204, 115253.	1.0	5
56	Fast and accurate lacunarity calculation for large 3D micro-CT datasets. Acta Materialia, 2021, 214, 116970.	3.8	15
57	M(II)Al4 Type Layered Double Hydroxides—Preparation Using Mechanochemical Route, Structural Characterization and Catalytic Application. Materials, 2021, 14, 4880.	1.3	5
58	Three-dimensional printing of complex graphite structures. Carbon, 2021, 181, 260-269.	5.4	10
59	Polyvinyl-Pyrrolidone-Coated Silver Nanoparticles—The Colloidal, Chemical, and Biological Consequences of Steric Stabilization under Biorelevant Conditions. International Journal of Molecular Sciences, 2021, 22, 8673.	1.8	25
60	Copper-Loaded Layered Bismuth Subcarbonate—Efficient Multifunctional Heterogeneous Catalyst for Concerted C–S/C–N Heterocyclization. ACS Applied Materials & Interfaces, 2021, 13, 42650-42661.	4.0	5
61	Chaetomium and Chaetomium-like Species from European Indoor Environments Include Dichotomopilus finlandicus sp. nov Pathogens, 2021, 10, 1133.	1.2	9
62	Nanoremediation: Tiny Objects Solving Huge Environmental Problems. Recent Patents on Nanotechnology, 2021, 15, 245-255.	0.7	1
63	Investigation of the efficiency of BiOI/BiOCl composite photocatalysts using UV, cool and warm white LED light sources - Photon efficiency, toxicity, reusability, matrix effect, and energy consumption. Chemosphere, 2021, 280, 130636.	4.2	19
64	Conventional or mechanochemically-aided intercalation of diclofenac and naproxen anions into the interlamellar space of CaFe-layered double hydroxides and their application as dermal drug delivery systems. Applied Clay Science, 2021, 212, 106233.	2.6	15
65	Combustion method combined with sonochemical step for synthesis of maghemite-supported catalysts for the hydrogenation of 2,4-dinitrotoluene. Catalysis Communications, 2021, 159, 106342.	1.6	6
66	Development of dexamethasone-loaded mixed polymeric micelles for nasal delivery. European Journal of Pharmaceutical Sciences, 2021, 166, 105960.	1.9	21
67	Size controlled Pt over mesoporous NiO nanocomposite catalysts: thermal catalysis vs. photocatalysis. Journal of Porous Materials, 2021, 28, 605-615.	1.3	2
68	Bioplastics and Carbon-Based Sustainable Materials, Components, and Devices: Toward Green Electronics. ACS Applied Materials & amp; Interfaces, 2021, 13, 49301-49312.	4.0	27
69	Optimization of layering technique and secondary structure analysis during the formulation of nanoparticles containing lysozyme by quality by design approach. PLoS ONE, 2021, 16, e0260603.	1.1	4
70	The Role of Electronegative and Electropositive Modifiers in the Adsorption and Decomposition of Acetaldehyde on $Rh(111)$ Surface. , 2021, 6, .		0
71	In Vitro Comparative Study of Solid Lipid and PLGA Nanoparticles Designed to Facilitate Nose-to-Brain Delivery of Insulin. International Journal of Molecular Sciences, 2021, 22, 13258.	1.8	21
72	Sonochemical Deposition of Palladium Nanoparticles Onto the Surface of N-Doped Carbon Nanotubes: A Simplified One-Step Catalyst Production Method. Catalysis Letters, 2020, 150, 505-513.	1.4	7

#	Article	IF	CITATIONS
73	Fast optical method for characterizing plasmonic nanoparticle adhesion on functionalized surfaces. Analytical and Bioanalytical Chemistry, 2020, 412, 3395-3404.	1.9	2
74	Luminescence and color properties of Ho3+ co-activated Sr4Al14O25: Eu2+, Dy3+ phosphors. Journal of Luminescence, 2020, 220, 116980.	1.5	3
75	Chronic responses of aerobic granules to the presence of graphene oxide in sequencing batch reactors. Journal of Hazardous Materials, 2020, 389, 121905.	6.5	21
76	β-Isocupreidinate‒CaAl-layered double hydroxide composites—heterogenized catalysts for asymmetric Michael addition. Molecular Catalysis, 2020, 482, 110675.	1.0	7
77	Layered double alkoxides a novel group of layered double hydroxides without water content. Materials Research Letters, 2020, 8, 68-74.	4.1	7
78	Ni–Zn–Al-Based Oxide/Spinel Nanostructures for High Performance, Methane-Selective CO2 Hydrogenation Reactions. Catalysis Letters, 2020, 150, 1527-1536.	1.4	11
79	Preparation of sulfur hydrophobized plasmonic photocatalyst towards durable superhydrophobic coating material. Journal of Materials Science and Technology, 2020, 41, 159-167.	5.6	8
80	Green and selective toluene oxidation–Knoevenagel-condensation domino reaction over Ce- and Bi-based CeBi mixed oxide mixtures. Journal of Catalysis, 2020, 381, 308-315.	3.1	24
81	On the effects of milling and thermal regeneration on the luminescence properties of Eu2+ and Dy3+ doped strontium aluminate phosphors. Journal of Luminescence, 2020, 219, 116917.	1.5	29
82	Squalenoylated Nanoparticle Pro-Drugs of Adjuvant Antitumor 11α-Hydroxyecdysteroid 2,3-Acetonides Act as Cytoprotective Agents Against Doxorubicin and Paclitaxel. Frontiers in Pharmacology, 2020, 11, 552088.	1.6	3
83	Mechanochemical and wet chemical syntheses of CaIn-layered double hydroxide and its performance in a transesterification reaction compared to those of other Ca2M(III) hydrocalumites (M: Al, Sc, V, Cr,) Tj ETQq1	1 0.7 8431	4 2g BT /Ovei
84	ZnO nanoparticles induce cell wall remodeling and modify ROS/ RNS signalling in roots of Brassica seedlings. Ecotoxicology and Environmental Safety, 2020, 206, 111158.	2.9	34
85	Phosphorus-loaded alumina supported nickel catalysts for CO2 hydrogenation: Ni2P/Ni5P12 drives activity. Molecular Catalysis, 2020, 494, 111113.	1.0	2
86	Electric and Photocatalytic Properties of Graphene Oxide Depending on the Degree of Its Reduction. Nanomaterials, 2020, 10, 2313.	1.9	5
87	A mineralogically-inspired silver–bismuth hybrid material: Structure, stability and application for catalytic benzyl alcohol dehydrogenations under continuous flow conditions. Molecular Catalysis, 2020, 498, 111263.	1.0	3
88	Quality by Design Based Formulation Study of Meloxicam-Loaded Polymeric Micelles for Intranasal Administration. Pharmaceutics, 2020, 12, 697.	2.0	36
89	The Structure and Thermal Properties of Solid Ternary Compounds Forming with Ca2+, Al3+ and Heptagluconate Ions. Molecules, 2020, 25, 4715.	1.7	1
90	<p>Presence of Titanium and Toxic Effects Observed in Rat Lungs, Kidneys, and Central Nervous System in vivo and in Cultured Astrocytes in vitro on Exposure by Titanium Dioxide Nanorods</p> . International Journal of Nanomedicine, 2020, Volume 15, 9939-9960.	3.3	12

#	Article	IF	CITATIONS
91	Dangling-to-Interstitial Oxygen Transition and Its Modifications of the Electronic Structure in Few-Layer Phosphorene. Journal of Physical Chemistry C, 2020, 124, 24066-24072.	1.5	8
92	Differential Precipitation of Mg(OH)2 from CaSO4·2H2O Using Citrate as Inhibitor—A Promising Concept for Reagent Recovery from MgSO4 Waste Streams. Molecules, 2020, 25, 5012.	1.7	6
93	Cu–Fe Incorporated Graphene-Oxide Nanocomposite as Highly Efficient Catalyst in the Degradation of Dichlorodiphenyltrichloroethane (DDT) from Aqueous Solution. Topics in Catalysis, 2020, 63, 1314-1324.	1.3	13
94	Grid-type transparent conductive thin films of carbon nanotubes as capacitive touch sensors. Nanotechnology, 2020, 31, 305303.	1.3	11
95	Temperatureâ€Dependent Electrical Transport Properties of Singleâ€Walled Carbon Nanotube Thin Films Prepared by Electrohydrodynamic Atomization Technique. Physica Status Solidi (A) Applications and Materials Science, 2020, 217, 2000029.	0.8	1
96	CulBiOI is an efficient novel catalyst in Ullmann-type CN couplings with wide scope—A rare non-photocatalyic application. Molecular Catalysis, 2020, 493, 111072.	1.0	3
97	Cost-effective ion-tuning of Birnessite structures for efficient ORR electrocatalysts. International Journal of Hydrogen Energy, 2020, 45, 16266-16276.	3.8	7
98	The Potassium-Induced Decomposition Pathway of HCOOH on Rh(111). Catalysts, 2020, 10, 675.	1.6	9
99	Adsorption of Azobenzene on Hexagonal Boron Nitride Nanomesh Supported by Rh(111). Journal of Physical Chemistry C, 2020, 124, 14182-14194.	1.5	6
100	One-pot mechanochemical ball milling synthesis of the MnO _x nanostructures as efficient catalysts for CO ₂ hydrogenation reactions. Physical Chemistry Chemical Physics, 2020, 22, 13999-14012.	1.3	15
101	Use of carbon paste electrode and modified by gold nanoparticles for selected macrolide antibiotics determination as standard and in pharmaceutical preparations. Journal of Electroanalytical Chemistry, 2020, 873, 114324.	1.9	14
102	Efficient visible-light piezophototronic activity of ZnO-Ag8S hybrid for degradation of organic dye molecule. Journal of Physics and Chemistry of Solids, 2020, 143, 109473.	1.9	16
103	Rh-induced Support Transformation and Rh Incorporation in Titanate Structures and Their Influence on Catalytic Activity. Catalysts, 2020, 10, 212.	1.6	10
104	Nitro-oxidative signalling induced by chemically synthetized zinc oxide nanoparticles (ZnO NPs) in Brassica species. Chemosphere, 2020, 251, 126419.	4.2	43
105	Porosity determination of nano- and sub-micron particles by single particle inductively coupled plasma mass spectrometry. Journal of Analytical Atomic Spectrometry, 2020, 35, 1139-1147.	1.6	18
106	Comparing the Adsorption Performance of Multiwalled Carbon Nanotubes Oxidized by Varying Degrees for Removal of Low Levels of Copper, Nickel and Chromium(VI) from Aqueous Solutions. Water (Switzerland), 2020, 12, 723.	1.2	30
107	Role of BrÃ,nsted and Lewis acidic sites in sulfonated Zr-MCM-41 for the catalytic reaction of cellulose into 5-hydroxymethyl furfural. Reaction Kinetics, Mechanisms and Catalysis, 2020, 130, 825-836.	0.8	14
108	Microcomputed tomography–based characterization of advanced materials: a review. Materials Today Advances, 2020, 8, 100084.	2.5	64

#	Article	IF	CITATIONS
109	Size-dependent activity of silver nanoparticles on the morphological switch and biofilm formation of opportunistic pathogenic yeasts. BMC Microbiology, 2020, 20, 176.	1.3	24
110	Sulfur nanoparticles transform montmorillonite into an inorganic surfactant applicable in thermoplastics processing. Polymer Testing, 2020, 85, 106419.	2.3	3
111	Catalytic activity of maghemite supported palladium catalyst in nitrobenzene hydrogenation. Reaction Kinetics, Mechanisms and Catalysis, 2020, 129, 107-116.	0.8	10
112	Core–shell nanoparticles suppress metastasis and modify the tumour-supportive activity of cancer-associated fibroblasts. Journal of Nanobiotechnology, 2020, 18, 18.	4.2	37
113	Selective transformation of ethanol to acetaldehyde catalyzed by Au/h-BN interface prepared on Rh(111) surface. Applied Catalysis A: General, 2020, 592, 117440.	2.2	10
114	Synergistic Radiosensitization by Gold Nanoparticles and the Histone Deacetylase Inhibitor SAHA in 2D and 3D Cancer Cell Cultures. Nanomaterials, 2020, 10, 158.	1.9	17
115	Ultrasound-Assisted Hydrazine Reduction Method for the Preparation of Nickel Nanoparticles, Physicochemical Characterization and Catalytic Application in Suzuki-Miyaura Cross-Coupling Reaction. Nanomaterials, 2020, 10, 632.	1.9	12
116	Ambient pressure CO2 hydrogenation over a cobalt/manganese-oxide nanostructured interface: A combined in situ and ex situ study. Journal of Catalysis, 2020, 386, 70-80.	3.1	34
117	Nitrogen doped carbon aerogel composites with TiO ₂ and ZnO prepared by atomic layer deposition. Journal of Materials Chemistry C, 2020, 8, 6891-6899.	2.7	10
118	Nature inspired solid–liquid phase amphibious adhesive. Soft Matter, 2020, 16, 5854-5860.	1.2	3
119	The use of functionalized titanate nanotubes as drug delivery systems. , 2020, , .		0
120	Rapid, trace-level direct cathodic voltammetric determination of dopamine by oxidized multiwalled carbon nanotube–modified carbon paste electrode in selected samples of pharmaceutical importance. Ionics, 2019, 25, 6093-6106.	1.2	11
121	Optimization of the Production Process and Product Quality of Titanate Nanotube–Drug Composites. Nanomaterials, 2019, 9, 1406.	1.9	3
122	Inhibition of protein phosphatase-1 and -2A by ellagitannins: structure-inhibitory potency relationships and influences on cellular systems. Journal of Enzyme Inhibition and Medicinal Chemistry, 2019, 34, 500-509.	2.5	5
123	Endoplasmic reticulum stress: major player in size-dependent inhibition of P-glycoprotein by silver nanoparticles in multidrug-resistant breast cancer cells. Journal of Nanobiotechnology, 2019, 17, 9.	4.2	52
124	<p>Silver nanoparticles: aggregation behavior in biorelevant conditions and its impact on biological activity</p> . International Journal of Nanomedicine, 2019, Volume 14, 667-687.	3.3	128
125	Synergetic of Pt Nanoparticles and H-ZSM-5 Zeolites for Efficient CO2 Activation: Role of Interfacial Sites in High Activity. Frontiers in Materials, 2019, 6, .	1.2	26
126	Noble-metal-free and Pt nanoparticles-loaded, mesoporous oxides as efficient catalysts for CO2 hydrogenation and dry reforming with methane. Journal of CO2 Utilization, 2019, 32, 106-118.	3.3	39

#	Article	IF	CITATIONS
127	Influencing the texture and morphological properties of layered double hydroxides with the most diluted solvent mixtures – The effect of 6–8 carbon alcohols and temperature. Colloids and Surfaces A: Physicochemical and Engineering Aspects, 2019, 574, 146-153.	2.3	4
128	Green synthesis and <i>in situ</i> immobilization of gold nanoparticles and their application for the reduction of <i>p</i> -nitrophenol in continuous-flow mode. RSC Advances, 2019, 9, 9193-9197.	1.7	9
129	Beyond Nanoparticles: The Role of Sub-nanosized Metal Species in Heterogeneous Catalysis. Catalysis Letters, 2019, 149, 1441.	1.4	15
130	Effects of ultrasonic irradiation on the synthesis, crystallization, thermal and dissolution behaviour of chloride-intercalated, co-precipitated CaFe-layered double hydroxide. Ultrasonics Sonochemistry, 2019, 55, 165-173.	3.8	12
131	Dissection of the regulatory role for the N-terminal domain in Candida albicans protein phosphatase Z1. PLoS ONE, 2019, 14, e0211426.	1.1	8
132	Placing Ni(II) Ions in Various Positions In/On Layered Double Hydroxides: Synthesis, Characterization and Testing in C–C Coupling Reactions. Catalysis Letters, 2019, 149, 2899-2905.	1.4	1
133	Structural reconstruction of mechanochemically disordered CaFe-layered double hydroxide. Applied Clay Science, 2019, 174, 138-145.	2.6	21
134	Lâ€Selectin Expression is Influenced by Phosphatase Activity in Chronic Lymphocytic Leukemia. Cytometry Part B - Clinical Cytometry, 2019, 96, 149-157.	0.7	7
135	Ultrasonically-assisted mechanochemical synthesis of zinc aluminate spinel from aluminium-rich layered double hydroxide. Journal of Solid State Chemistry, 2019, 272, 227-233.	1.4	8
136	Aging Impairs Cerebrovascular Reactivity at Preserved Resting Cerebral Arteriolar Tone and Vascular Density in the Laboratory Rat. Frontiers in Aging Neuroscience, 2019, 11, 301.	1.7	12
137	Novel route to synthesize CaAl- and MgAl-layered double hydroxides with highly regular morphology. Journal of Sol-Gel Science and Technology, 2019, 89, 844-851.	1.1	10
138	Mechanochemically modified hydrazine reduction method for the synthesis of nickel nanoparticles and their catalytic activities in the Suzuki–Miyaura cross-coupling reaction. Reaction Kinetics, Mechanisms and Catalysis, 2019, 126, 857-868.	0.8	8
139	Designed Pt Promoted 3D Mesoporous Co3O4 Catalyst in CO2 Hydrogenation. Journal of Nanoscience and Nanotechnology, 2019, 19, 436-441.	0.9	5
140	Gold Size Effect in the Thermal-Induced Reaction of CO ₂ and H ₂ on Titania- and Titanate Nanotube-Supported Gold Catalysts. Journal of Nanoscience and Nanotechnology, 2019, 19, 470-477.	0.9	13
141	Size-Dependent H ₂ Sensing Over Supported Pt Nanoparticles. Journal of Nanoscience and Nanotechnology, 2019, 19, 459-464.	0.9	2
142	Co(II)-amino acid–CaAl-layered double hydroxide composites–ÂConstruction and characterization. Journal of Molecular Structure, 2019, 1179, 263-268.	1.8	5
143	Electrical and Photoelectrical Characteristics of ѕSi/Porous–Si/CdS Heterojunctions. Russian Physics Journal, 2019, 61, 1660-1666.	0.2	11
144	Effects of medium and nickel salt source in the synthesis and catalytic performance of nano-sized nickel in the Suzuki-Miyaura cross-coupling reaction. Reaction Kinetics, Mechanisms and Catalysis, 2019, 126, 841-855.	0.8	1

#	Article	IF	CITATIONS
145	Trace level voltammetric determination of Zn(II) in selected nutrition related samples by bismuth-oxychloride-multiwalled carbon nanotube composite based electrode. Microchemical Journal, 2019, 146, 178-186.	2.3	17
146	The aggregation behaviour of 2H-imidazole-2-thione derivatives in solution, the solid state and over polycrystalline gold surface. Journal of Molecular Structure, 2019, 1180, 26-30.	1.8	0
147	Noble-Metal-Free Iron Nitride/Nitrogen-Doped Graphene Composite for the Oxygen Reduction Reaction. ACS Omega, 2019, 4, 130-139.	1.6	29
148	Outstanding Activity and Selectivity of Controlled Size Pt Nanoparticles Over WO ₃ Nanowires in Ethanol Decomposition Reaction. Journal of Nanoscience and Nanotechnology, 2019, 19, 478-483.	0.9	6
149	Preparation of photocatalytic thin films with composition dependent wetting properties and self-healing ability. Catalysis Today, 2019, 328, 85-90.	2.2	13
150	Amperometric Determination of Glucose in White Grape and in Tablets as Ingredient by Screen-Printed Electrode Modified with Glucose Oxidase and Composite of Platinum and Multiwalled Carbon Nanotubes. Food Analytical Methods, 2019, 12, 570-580.	1.3	13
151	Ball Milling of Copper Powder Under Dry and Surfactant-Assisted Conditions—On the Way Towards Cu/Cu ₂ O Nanocatalyst. Journal of Nanoscience and Nanotechnology, 2019, 19, 389-394.	0.9	9
152	Effect of Particle Restructuring During Reduction Processes Over Polydopamine-Supported Pd Nanoparticles. Journal of Nanoscience and Nanotechnology, 2019, 19, 484-491.	0.9	6
153	The Synthesis and Use of Nano Nickel Catalysts. Journal of Nanoscience and Nanotechnology, 2019, 19, 453-458.	0.9	7
154	Composition-Dependent Optical and Photoelectrochemical Behavior of Antimony Oxide Iodides. Journal of the Electrochemical Society, 2019, 166, H3202-H3207.	1.3	2
155	Aralkyl selenoglycosides and related selenosugars in acetylated form activate protein phosphatase-1 and -2A. Bioorganic and Medicinal Chemistry, 2018, 26, 1875-1884.	1.4	8
156	In Situ DRIFTS and NAP-XPS Exploration of the Complexity of CO ₂ Hydrogenation over Size-Controlled Pt Nanoparticles Supported on Mesoporous NiO. Journal of Physical Chemistry C, 2018, 122, 5553-5565.	1.5	72
157	Hydrogen evolution in the photocatalytic reaction between methane and water in the presence of CO2 on titanate and titania supported Rh and Au catalysts. Topics in Catalysis, 2018, 61, 875-888.	1.3	19
158	Effect of sonication time on the synthesis of the CdS nanoparticle based multiwall carbon nanotube – maleic anhydride – 1-octene nanocomposites. Fullerenes Nanotubes and Carbon Nanostructures, 2018, 26, 255-262.	1.0	8
159	Thermo-optical properties of residential coals and combustion aerosols. Atmospheric Environment, 2018, 178, 118-128.	1.9	19
160	Reforming of ethanol on Co/Al2O3 catalysts reduced at different temperatures. Journal of Catalysis, 2018, 358, 118-130.	3.1	43
161	A mineralogically-inspired silver–bismuth hybrid material: an efficient heterogeneous catalyst for the direct synthesis of nitriles from terminal alkynes. Green Chemistry, 2018, 20, 1007-1019.	4.6	16
162	Diversity of Pd-Cu active sites supported on pristine carbon nanotubes in terms of water denitration structure sensitivity. Applied Catalysis A: General, 2018, 559, 187-194.	2.2	12

#	Article	IF	CITATIONS
163	One step synthesis of chlorine-free Pt/Nitrogen-doped graphene composite for oxygen reduction reaction. Carbon, 2018, 133, 90-100.	5.4	25
164	Green synthesis of gold nanoparticles by thermophilic filamentous fungi. Scientific Reports, 2018, 8, 3943.	1.6	261
165	Syntheses, characterization and catalytic activities of CaAl-layered double hydroxide intercalated Fe(III)-amino acid complexes. Catalysis Today, 2018, 306, 42-50.	2.2	10
166	Development and characterization of multi-element doped hydroxyapatite bioceramic coatings on metallic implants for orthopedic applications. Boletin De La Sociedad Espanola De Ceramica Y Vidrio, 2018, 57, 55-65.	0.9	44
167	Pulse electrodeposition and characterization of non-continuous, multi-element-doped hydroxyapatite bioceramic coatings. Journal of Solid State Electrochemistry, 2018, 22, 555-566.	1.2	11
168	Allyl-Isothiocyanate and Microcystin-LR Reveal the Protein Phosphatase Mediated Regulation of Metaphase-Anaphase Transition in Vicia faba. Frontiers in Plant Science, 2018, 9, 1823.	1.7	4
169	Comment on "Causation or only correlation? Application of causal inference graphs for evaluating causality in nano-QSAR models―by N. Sizochenko, A. Gajewicz, J. Leszczynski and T. Puzyn, <i>Nanoscale</i> , 2016, 8, 7203. Nanoscale, 2018, 10, 20863-20866.	2.8	3
170	Pulmonary impact of titanium dioxide nanorods: examination of nanorod-exposed rat lungs and human alveolar cells. International Journal of Nanomedicine, 2018, Volume 13, 7061-7077.	3.3	8
171	Investigation of the Compressibility and Compactibility of Titanate Nanotube-API Composites. Materials, 2018, 11, 2582.	1.3	3
172	Quantitative Tracking of the Oxidation of Black Phosphorus in the Few-Layer Regime. ACS Omega, 2018, 3, 12482-12488.	1.6	31
173	Development and Application of Carbon‣ayer‣tabilized, Nitrogenâ€Doped, Bamboo‣ike Carbon Nanotube Catalysts in CO ₂ Hydrogenation. ChemistryOpen, 2018, 7, 789-796.	0.9	9
174	Au–Rh Surface Structures on Rh(111): DFT Insights into the Formation of an Ordered Surface Alloy. Journal of Physical Chemistry C, 2018, 122, 22435-22447.	1.5	5
175	Reaction and Diffusion Paths of Water and Hydrogen on Rh Covered Black Titania. Topics in Catalysis, 2018, 61, 1362-1374.	1.3	1
176	Effect of Gold on the Adsorption Properties of Acetaldehyde on Clean and h-BN Covered Rh(111) Surface. Topics in Catalysis, 2018, 61, 1247-1256.	1.3	9
177	Tailoring the hexagonal boron nitride nanomesh on Rh(111) with gold. Physical Chemistry Chemical Physics, 2018, 20, 15473-15485.	1.3	17
178	Co4N/nitrogen-doped graphene: A non-noble metal oxygen reduction electrocatalyst for alkaline fuel cells. Applied Catalysis B: Environmental, 2018, 237, 826-834.	10.8	80
179	Chemical characterization of laboratory-generated tar ball particles. Atmospheric Chemistry and Physics, 2018, 18, 10407-10418.	1.9	24
180	Biosynthesized silver and gold nanoparticles are potent antimycotics against opportunistic pathogenic yeasts and dermatophytes. International Journal of Nanomedicine, 2018, Volume 13, 695-703.	3.3	78

#	Article	IF	CITATIONS
181	Tuning the Activity and Selectivity of Phenylacetylene Hydrosilylation with Triethylsilane in the Liquid Phase over Size Controlled Pt Nanoparticles. Catalysts, 2018, 8, 22.	1.6	7
182	Myosin phosphatase accelerates cutaneous wound healing by regulating migration and differentiation of epidermal keratinocytes via Akt signaling pathway in human and murine skin. Biochimica Et Biophysica Acta - Molecular Basis of Disease, 2018, 1864, 3268-3280.	1.8	6
183	Morphology Conserving High Efficiency Nitrogen Doping of Titanate Nanotubes by NH3 Plasma. Topics in Catalysis, 2018, 61, 1263-1273.	1.3	5
184	Ag or Au Nanoparticles Decorated Multiwalled Carbon Nanotubes Coated Carbon Paste Electrodes for Amperometric Determination of H2O2. Topics in Catalysis, 2018, 61, 1350-1361.	1.3	14
185	Rapid amperometric determination of H2O2 by a Pt nanoparticle/Vulcan XC72 composite-coated carbon paste electrode in disinfection and contact lens solutions. Monatshefte Für Chemie, 2018, 149, 1727-1738.	0.9	6
186	A novel carbon tipped single micro-optrode for combined optogenetics and electrophysiology. PLoS ONE, 2018, 13, e0193836.	1.1	19
187	Acetone improves the topographical homogeneity of liquid phase exfoliated few-layer black phosphorus flakes. Nanotechnology, 2018, 29, 365303.	1.3	16
188	Ultrasonically-enhanced preparation, characterization of CaFe-layered double hydroxides with various interlayer halide, azide and oxo anions (CO32â^', NO3â^', ClO4â^'). Ultrasonics Sonochemistry, 2018, 40, 853-860.	3.8	27
189	Fabrication and characterization of c-Si/porous-Si/CdS/ZnxCd1-xO heterojunctions for applications in nanostructured solar cells. Photonics Letters of Poland, 2018, 10, 73.	0.2	1
190	Potential solvents in coupling reactions catalyzed by Cu(II)Fe(III)-layered double hydroxide in a continuous-flow reactor. Reaction Kinetics, Mechanisms and Catalysis, 2017, 121, 345-351.	0.8	2
191	Systematic comparison of saturation effects and afterglow properties of Sr4Al14O25:Eu, Dy phosphor excited by alpha and beta ionizing sources and UV light. Journal of Molecular Structure, 2017, 1140, 89-98.	1.8	5
192	Borate-containing layered double hydroxide composites: synthesis, characterization and application as catalysts in the Beckmann rearrangement reaction of cyclohexanone oxime. Reaction Kinetics, Mechanisms and Catalysis, 2017, 121, 241-254.	0.8	2
193	Voltammetric behavior and determination of the macrolide antibiotics azithromycin, clarithromycin and roxithromycin at a renewable silver – amalgam film electrode. Electrochimica Acta, 2017, 229, 334-344.	2.6	32
194	Silica-Based Catalyst Supports Are Inert, Are They Not?: Striking Differences in Ethanol Decomposition Reaction Originated from Meso- and Surface-Fine-Structure Evidenced by Small-Angle X-ray Scattering. Journal of Physical Chemistry C, 2017, 121, 5130-5136.	1.5	12
195	pH-regulated antimony oxychloride nanoparticle formation on titanium oxide nanostructures: a photocatalytically active heterojunction. CrystEngComm, 2017, 19, 1408-1416.	1.3	3
196	Mn(II)-containing layered double hydroxide composites: synthesis, characterization and an application in Ullmann diaryl etherification. Reaction Kinetics, Mechanisms and Catalysis, 2017, 121, 175-184.	0.8	2
197	Exploring Pd/Al2O3 Catalysed Redox Isomerisation of Allyl Alcohol as a Platform to Create Structural Diversity. Catalysis Letters, 2017, 147, 1834-1843.	1.4	3
198	Adsorption, polymerization and decomposition of acetaldehyde on clean and carbon-covered Rh(111) surfaces. Surface Science, 2017, 664, 129-136.	0.8	12

#	Article	IF	CITATIONS
199	Kinetic, equilibrium and thermodynamic studies of thiamethoxam adsorption by multi-walled carbon nanotubes. International Journal of Environmental Science and Technology, 2017, 14, 1297-1306.	1.8	10
200	Screen-printed enzymatic glucose biosensor based on a composite made from multiwalled carbon nanotubes and palladium containing particles. Mikrochimica Acta, 2017, 184, 1987-1996.	2.5	18
201	Determination of the platinum concentration of a Pt/silica nanocomposite decorated with ultra small Pt nanoparticles using single particle inductively coupled plasma mass spectrometry. Journal of Analytical Atomic Spectrometry, 2017, 32, 996-1003.	1.6	21
202	Photoelectrochemistry by Design: Tailoring the Nanoscale Structure of Pt/NiO Composites Leads to Enhanced Photoelectrochemical Hydrogen Evolution Performance. Journal of Physical Chemistry C, 2017, 121, 12148-12158.	1.5	20
203	Interplay of myosin phosphatase and protein phosphatase-2A in the regulation of endothelial nitric-oxide synthase phosphorylation and nitric oxide production. Scientific Reports, 2017, 7, 44698.	1.6	16
204	Titania nanotube stabilized BiOCl nanoparticles in visible-light photocatalysis. RSC Advances, 2017, 7, 16410-16422.	1.7	15
205	The promotion of CO dissociation by molybdenum oxide overlayers on rhodium. Surface Science, 2017, 657, 1-9.	0.8	5
206	Physicochemical characterisation and investigation of the bonding mechanisms of API-titanate nanotube composites as new drug carrier systems. International Journal of Pharmaceutics, 2017, 518, 119-129.	2.6	10
207	Room temperature ethanol sensor with sub-ppm detection limit: Improving the optical response by using mesoporous silica foam. Sensors and Actuators B: Chemical, 2017, 243, 1205-1213.	4.0	18
208	Structure and stability of boron doped titanate nanotubes and nanowires. Vacuum, 2017, 138, 120-124.	1.6	13
209	Thin-walled nanoscrolls by multi-step intercalation from tubular halloysite-10 Ã and its rearrangement upon peroxide treatment. Applied Surface Science, 2017, 399, 245-254.	3.1	16
210	From nicotinate-containing layered double hydroxides (LDHs) to NAD coenzyme–LDH nanocomposites – Syntheses and structural characterization by various spectroscopic methods. Journal of Molecular Structure, 2017, 1140, 39-45.	1.8	2
211	Synthesis, characterization and photocatalytic activity of crystalline Mn(II)Cr(III)-layered double hydroxide. Catalysis Today, 2017, 284, 195-201.	2.2	26
212	Molybdenum anchoring effect in Fe–Mo/MgO catalyst for multiwalled carbon nanotube synthesis. Reaction Kinetics, Mechanisms and Catalysis, 2017, 122, 775-791.	0.8	11
213	Nitridation of one-dimensional tungsten oxide nanostructures: Changes in structure and photoactivity. Electrochimica Acta, 2017, 256, 299-306.	2.6	14
214	Facile synthesis route of graphene-like structures from multiwall carbon nanotubes. Fullerenes Nanotubes and Carbon Nanostructures, 2017, 25, 540-544.	1.0	8
215	Mixed Oxides Without Added Noble Metals Derived from Layered Double Hydroxides of the Hydrotalcite Type in the Hydrodechlorination Reaction of Trichloroethylene. Catalysis Letters, 2017, 147, 2910-2919.	1.4	3
216	Comparative study on the rheological properties and tablettability of various APIs and their composites with titanate nanotubes. Powder Technology, 2017, 321, 419-427.	2.1	2

#	Article	IF	CITATIONS
217	Ni-Amino Acid–CaAl-Layered Double Hydroxide Composites: Construction, Characterization and Catalytic Properties in Oxidative Transformations. Topics in Catalysis, 2017, 60, 1429-1438.	1.3	7
218	Portable cyber-physical system for indoor and outdoor gas sensing. Sensors and Actuators B: Chemical, 2017, 252, 983-990.	4.0	15
219	Photoelectrical response of mesoporous nickel oxide decorated with size controlled platinum nanoparticles under argon and oxygen gas. Catalysis Today, 2017, 284, 37-43.	2.2	9
220	On-chip integrated vertically aligned carbon nanotube based super- and pseudocapacitors. Scientific Reports, 2017, 7, 16594.	1.6	30
221	Biological activity of green-synthesized silver nanoparticles depends on the applied natural extracts: a comprehensive study. International Journal of Nanomedicine, 2017, Volume 12, 871-883.	3.3	120
222	Localized growth of carbon nanotubes via lithographic fabrication of metallic deposits. Beilstein Journal of Nanotechnology, 2017, 8, 2592-2605.	1.5	3
223	Propionic Acid Produced by Propionibacterium acnes Strains ContriÂbutes to Their Pathogenicity. Acta Dermato-Venereologica, 2016, 96, 43-49.	0.6	46
224	Modulating chromatin structure and DNA accessibility by deacetylase inhibition enhances the anti-cancer activity of silver nanoparticles. Colloids and Surfaces B: Biointerfaces, 2016, 146, 670-677.	2.5	38
225	Silver nanoparticles defeat p53-positive and p53-negative osteosarcoma cells by triggering mitochondrial stress and apoptosis. Scientific Reports, 2016, 6, 27902.	1.6	94
226	Ultrasound-enhanced milling in the synthesis of phase-pure, highly crystalline ZnAl-layered double hydroxide of low Zn(II) content. Particuology, 2016, 27, 29-33.	2.0	20
227	Characterisation of diesel particulate emission from engines using commercial diesel and biofuels. Atmospheric Environment, 2016, 134, 109-120.	1.9	20
228	Hydrodynamic chronoamperometric determination of hydrogen peroxide using carbon paste electrodes coated by multiwalled carbon nanotubes decorated with MnO2 or Pt particles. Sensors and Actuators B: Chemical, 2016, 233, 83-92.	4.0	33
229	Synthesis of high-quality, well-characterized CaAlFe-layered triple hydroxide with the combination of dry-milling and ultrasonic irradiation in aqueous solution at elevated temperature. Ultrasonics Sonochemistry, 2016, 32, 173-180.	3.8	16
230	Experimental validation of the Burgio–Rojac model of planetary ball milling by the length control of multiwall carbon nanotubes. Carbon, 2016, 105, 615-621.	5.4	8
231	Microcystin-LR induces mitotic spindle assembly disorders in Vicia faba by protein phosphatase inhibition and not reactive oxygen species induction. Journal of Plant Physiology, 2016, 199, 1-11.	1.6	18
232	Characterization and Catalytic Activity of Different Carbon Supported Pd Nanocomposites. Catalysis Letters, 2016, 146, 2268-2277.	1.4	8
233	Molecular Insights into the Fungus-Specific Serine/Threonine Protein Phosphatase Z1 in Candida albicans. MBio, 2016, 7, .	1.8	22
234	The growth and thermal properties of Au deposited on Rh(111): formation of an ordered surface alloy. Physical Chemistry Chemical Physics, 2016, 18, 25230-25240.	1.3	9

#	Article	IF	CITATIONS
235	Understanding the role of post-CCVD synthetic impurities, functional groups and functionalization-based oxidation debris on the behaviour of carbon nanotubes as a catalyst support in cyclohexene hydrogenation over Pd nanoparticles. RSC Advances, 2016, 6, 88538-88545.	1.7	2
236	Sorption Behaviour of Trichlorobenzenes and Polycyclic Aromatic Hydrocarbons in the Absence or Presence of Carbon Nanotubes in the Aquatic Environment. Water, Air, and Soil Pollution, 2016, 227, 1.	1.1	6
237	Photo-induced reactions in the CO 2 -methane system on titanate nanotubes modified with Au and Rh nanoparticles. Applied Catalysis B: Environmental, 2016, 199, 473-484.	10.8	108
238	The Effect of Rh on the Interaction of Co with Al2O3 and CeO2 Supports. Catalysis Letters, 2016, 146, 1800-1807.	1.4	14
239	Estimation of the solubility product of hydrocalumite–hydroxide, a layered double hydroxide with the formula of [Ca2Al(OH)6]OH·nH2O. Journal of Physics and Chemistry of Solids, 2016, 98, 167-173.	1.9	11
240	Qualitative Discrimination Analysis of Coals Based on Their Laser-Induced Breakdown Spectra. Energy & Fuels, 2016, 30, 10306-10313.	2.5	14
241	A novel WS2 nanowire-nanoflake hybrid material synthesized from WO3 nanowires in sulfur vapor. Scientific Reports, 2016, 6, 25610.	1.6	21
242	Catalytic Hydrogenation of d-Xylose Over Ru Decorated Carbon Foam Catalyst in a SpinChem® Rotating Bed Reactor. Topics in Catalysis, 2016, 59, 1165-1177.	1.3	40
243	Albumin adsorption study onto hydroxyapatite-multiwall carbon nanotube based composites. Materials Chemistry and Physics, 2016, 180, 314-325.	2.0	8
244	Cu(II)-amino acid–CaAl-layered double hydroxide complexes, recyclable, efficient catalysts in various oxidative transformations. Journal of Molecular Catalysis A, 2016, 423, 49-60.	4.8	18
245	Atomic scale characterization and surface chemistry of metal modified titanate nanotubes and nanowires. Surface Science Reports, 2016, 71, 473-546.	3.8	96
246	Ion exchange defines the biological activity of titanate nanotubes. Journal of Basic Microbiology, 2016, 56, 557-565.	1.8	13
247	Mn(II)–amino acid complexes intercalated in CaAl-layered double hydroxide – Well-characterized, highly efficient, recyclable oxidation catalysts. Journal of Catalysis, 2016, 335, 125-134.	3.1	42
248	Mesoporous carbon-supported Pd nanoparticles with high specific surface area for cyclohexene hydrogenation: Outstanding catalytic activity of NaOH-treated catalysts. Surface Science, 2016, 648, 114-119.	0.8	9
249	Mechanochemical synthesis and intercalation of Ca(II)Fe(III)-layered double hydroxides. Journal of Solid State Chemistry, 2016, 233, 236-243.	1.4	28
250	Environmentally Benign Synthesis Methods of Zero-Valent Iron Nanoparticles. ACS Sustainable Chemistry and Engineering, 2016, 4, 291-297.	3.2	70
251	Silver nanoparticles modulate ABC transporter activity and enhance chemotherapy in multidrug resistant cancer. Nanomedicine: Nanotechnology, Biology, and Medicine, 2016, 12, 601-610.	1.7	54
252	Impact of the morphology and reactivity of nanoscale zero-valent iron (NZVI) on dechlorinating bacteria. Water Research, 2016, 95, 165-173.	5.3	43

#	Article	IF	CITATIONS
253	Removal of As(III) and Cr(VI) from aqueous solutions using "green―zero-valent iron nanoparticles produced by oak, mulberry and cherry leaf extracts. Ecological Engineering, 2016, 90, 42-49.	1.6	129
254	Ultrasonically-enhanced mechanochemical synthesis of CaAl-layered double hydroxides intercalated by a variety of inorganic anions. Ultrasonics Sonochemistry, 2016, 31, 409-416.	3.8	39
255	Flow-driven morphology control in the cobalt–oxalate system. CrystEngComm, 2016, 18, 2057-2064.	1.3	20
256	Stability and Temperature-Induced Agglomeration of Rh Nanoparticles Supported by CeO ₂ . Langmuir, 2016, 32, 2761-2770.	1.6	47
257	Synthesis and characterization of CdS nanocrystals in Maleic anhydride–Octene-1–Vinylbutyl Ether terpolymer matrix. Physica E: Low-Dimensional Systems and Nanostructures, 2016, 81, 150-155.	1.3	3
258	Voltammetric behavior of erythromycin ethylsuccinate at a renewable silver-amalgam film electrode and its determination in urine and in a pharmaceutical preparation. Electrochimica Acta, 2016, 191, 44-54.	2.6	20
259	Size-Dependent Toxicity Differences of Intratracheally Instilled Manganese Oxide Nanoparticles: Conclusions of a Subacute Animal Experiment. Biological Trace Element Research, 2016, 171, 156-166.	1.9	26
260	Analysis of Two Putative Candida albicans Phosphopantothenoylcysteine Decarboxylase / Protein Phosphatase Z Regulatory Subunits Reveals an Unexpected Distribution of Functional Roles. PLoS ONE, 2016, 11, e0160965.	1.1	11
261	Adsorption of chlorinated phenols on multiwalled carbon nanotubes. RSC Advances, 2015, 5, 24920-24929.	1.7	22
262	Unveiling the Role of CNTs in the Phase Formation of One-Dimensional Ferroelectrics. Langmuir, 2015, 31, 6713-6720.	1.6	2
263	Rh and Au deposited on ultrathin TiO~1.2 film formed on Rh(111) facets and the effects of CO exposure. Surface Science, 2015, 641, 300-304.	0.8	10
264	Trace level voltammetric determination of lead and cadmium in sediment pore water by a bismuth-oxychloride particle-multiwalled carbon nanotube composite modified glassy carbon electrode. Talanta, 2015, 134, 640-649.	2.9	103
265	Synthesis and characterization of CdS nanoparticle based multiwall carbon nanotube–maleic anhydride–1-octene nanocomposites. Physica E: Low-Dimensional Systems and Nanostructures, 2015, 69, 212-218.	1.3	13
266	Bimetallic Fe/Mo–SiO2 aerogel catalysts for catalytic carbon vapour deposition production of carbon nanotubes. Journal of Sol-Gel Science and Technology, 2015, 73, 379-388.	1.1	10
267	LEIS and XPS investigation into the growth of cerium and cerium dioxide on Cu(111). Physical Chemistry Chemical Physics, 2015, 17, 5124-5132.	1.3	25
268	Visible light induced photocatalytic activity of TiO2 nanowires photosensitized with CdSe quantum dots. Reaction Kinetics, Mechanisms and Catalysis, 2015, 115, 143-157.	0.8	4
269	Enhanced dispersion and the reactivity of atomically thin Rh layers supported by molybdenum oxide films. Surface Science, 2015, 641, 60-67.	0.8	3
270	Evaluation and comparison of the ammonia adsorption capacity of titanosilicates ETS-4 and ETS-10 and aluminotitanosilicates ETAS-4 and ETAS-10. Journal of Thermal Analysis and Calorimetry, 2015, 122, 1257-1267.	2.0	20

#	Article	IF	CITATIONS
271	Investigation of the adsorption properties of borazine and characterisation of boron nitride on Rh(1 1) Tj ETQq1 1	0.784314 3.1	l rgBT /Ovei
272	Optimization of thiamethoxam adsorption parameters using multi-walled carbon nanotubes by means of fractional factorial design. Chemosphere, 2015, 141, 87-93.	4.2	36
273	Determination of H2O2 by MnO2 modified screen printed carbon electrode during Fenton and visible light-assisted photo-Fenton based removal of acetamiprid from water. Journal of Electroanalytical Chemistry, 2015, 755, 77-86.	1.9	19
274	Visible light activation photocatalytic performance of PbSe quantum dot sensitized TiO2 Nanowires. Applied Catalysis B: Environmental, 2015, 179, 583-588.	10.8	26
275	Optimisation of the synthesis parameters of mechanochemically prepared CaAl-layered double hydroxide. Applied Clay Science, 2015, 112-113, 94-99.	2.6	38
276	Microphysical properties of carbonaceous aerosol particles generated by laser ablation of a graphite target. Atmospheric Measurement Techniques, 2015, 8, 1207-1215.	1.2	13
277	Structure-Independent Proton Transport in Cerium(III) Phosphate Nanowires. ACS Applied Materials & Interfaces, 2015, 7, 9947-9956.	4.0	16
278	Layered titanate nanostructures: perspectives for industrial exploitation. Translational Materials Research, 2015, 2, 015003.	1.2	35
279	The Interaction of Cobalt with CeO ₂ (111) Prepared on Cu(111). Journal of Physical Chemistry C, 2015, 119, 9324-9333.	1.5	32
280	Facile synthesis of CuS nanoparticles deposited on polymer nanocomposite foam and their effects on microstructural and optical properties. European Polymer Journal, 2015, 68, 47-56.	2.6	16
281	Functionalized boron nitride porous solids. RSC Advances, 2015, 5, 93964-93968.	1.7	89
282	A simple method to control the formation of cerium phosphate architectures. CrystEngComm, 2015, 17, 8477-8485.	1.3	20
283	Probing the interaction of Rh, Co and bimetallic Rh–Co nanoparticles with the CeO ₂ support: catalytic materials for alternative energy generation. Physical Chemistry Chemical Physics, 2015, 17, 27154-27166.	1.3	52
284	Synthesis and 1-butene hydrogenation activity of platinum decorated bamboo-shaped multiwall carbon nanotubes. Reaction Kinetics, Mechanisms and Catalysis, 2015, 116, 371-383.	0.8	7
285	Facile synthesis of nanostructured carbon materials over RANEY® nickel catalyst films printed on Al2O3 and SiO2 substrates. Journal of Materials Chemistry C, 2015, 3, 1823-1829.	2.7	2
286	Thermal decomposition and reconstruction of CaFe-layered double hydroxide studied by X-ray diffractometry and 57Fe Mössbauer spectroscopy. Journal of Molecular Structure, 2015, 1090, 19-24.	1.8	11
287	Protein phosphatase-1 is involved in the maintenance of normal homeostasis and in UVA irradiation-induced pathological alterations in HaCaT cells and in mouse skin. Biochimica Et Biophysica Acta - Molecular Basis of Disease, 2015, 1852, 22-33.	1.8	7
288	Synthesis and characterization of composition-gradient based CdxZn1â^'xSeyS1â^'y heterostructured quantum dots. Reaction Kinetics, Mechanisms and Catalysis, 2015, 115, 129-141.	0.8	1

#	Article	IF	CITATIONS
289	The catalytic epoxidation of 2-cyclohexen-1-one over uncalcined layered double hydroxides using various solvents. Catalysis Today, 2015, 241, 231-236.	2.2	13
290	Decoration of Titanate Nanowires and Nanotubes by Gold Nanoparticles: XPS, HRTEM and XRD Characterization. E-Journal of Surface Science and Nanotechnology, 2014, 12, 252-258.	0.1	10
291	Mechanochemically assisted synthesis of pristine Ca(II)Sn(IV)-layered double hydroxides and their amino acid intercalated nanocomposites. Journal of Materials Science, 2014, 49, 8478-8486.	1.7	37
292	Photocatalytic H2 Production Using Pt-TiO2 in the Presence of Oxalic Acid: Influence of the Noble Metal Size and the Carrier Gas Flow Rate. Materials, 2014, 7, 7022-7038.	1.3	18
293	Gas Sensing and Thermal Transport Through Carbon-Nanotube-Based Nanodevices. Challenges and Advances in Computational Chemistry and Physics, 2014, , 99-136.	0.6	1
294	Photocatalytic H2 Evolution Using Different Commercial TiO2 Catalysts Deposited with Finely Size-Tailored Au Nanoparticles: Critical Dependence on Au Particle Size. Materials, 2014, 7, 7615-7633.	1.3	13
295	Preparation and Investigation of p-GaAs/n-Cd1-xZnxS1-yTey Heterojunctions Deposited by Electrochemical Deposition. Journal of Solar Energy Engineering, Transactions of the ASME, 2014, 136,	1.1	3
296	Growth of Gold on a Pinwheel TiOâ^¼1.2 Encapsulation Film Prepared on Rhodium Nanocrystallites. Langmuir, 2014, 30, 14545-14554.	1.6	8
297	Exploiting the ion-exchange ability of titanate nanotubes in a model water softening process. Chemical Physics Letters, 2014, 591, 161-165.	1.2	22
298	Photocatalytic activity of nitrogen-doped TiO2-based nanowires: a photo-assisted Kelvin probe force microscopy study. Journal of Nanoparticle Research, 2014, 16, 1.	0.8	11
299	Investigation of the Cytotoxic Effects of Titanate Nanotubes on Caco-2 Cells. AAPS PharmSciTech, 2014, 15, 858-861.	1.5	15
300	Mössbauer and XRD study of intercalated CaFe-layered double hydroxides. Hyperfine Interactions, 2014, 226, 171-179.	0.2	4
301	Search for a Raney-Ni type catalyst efficient in the transformation of excess glycerol into more valuable products. Catalysis Communications, 2014, 43, 116-120.	1.6	9
302	Effect of a Gold Cover Layer on the Encapsulation of Rhodium by Titanium Oxides on Titanium Dioxide(110). Journal of Physical Chemistry C, 2014, 118, 12340-12352.	1.5	15
303	Carbon nanotube-layered double hydroxide nanocomposites. Chemical Papers, 2014, 68, .	1.0	6
304	Titania nanofibers in gypsum composites: an antibacterial and cytotoxicology study. Journal of Materials Chemistry B, 2014, 2, 1307.	2.9	19
305	Synthesis and properties of CaAl-layered double hydroxides of hydrocalumite-type. Chemical Papers, 2014, 68, .	1.0	24
306	Influence of gold additives on the stability and phase transformation of titanate nanostructures. Physical Chemistry Chemical Physics, 2014, 16, 26786-26797.	1.3	33

#	Article	IF	CITATIONS
307	Iron/cobalt-SBA-16 cubic mesoporous composites as catalysts for the production of multi-walled carbon nanotubes. Journal of Porous Materials, 2014, 21, 1123-1131.	1.3	3
308	Green synthesis of biomimetic CePO ₄ :Tb nanostructures using the simplest morphology control. RSC Advances, 2014, 4, 49879-49887.	1.7	9
309	Low-temperature conversion of titanate nanotubes into nitrogen-doped TiO ₂ nanoparticles. CrystEngComm, 2014, 16, 7486-7492.	1.3	19
310	Toxic metal immobilization in contaminated sediment using bentonite- and kaolinite-supported nano zero-valent iron. Journal of Nanoparticle Research, 2014, 16, 1.	0.8	35
311	Synthesis and characterization of polyvinyl alcohol based multiwalled carbon nanotube nanocomposites. Physica E: Low-Dimensional Systems and Nanostructures, 2014, 61, 129-134.	1.3	58
312	Dry reforming of CH4 on Rh doped Co/Al2O3 catalysts. Catalysis Today, 2014, 228, 123-130.	2.2	49
313	Effects of Support and Rh Additive on Co-Based Catalysts in the Ethanol Steam Reforming Reaction. ACS Catalysis, 2014, 4, 1205-1218.	5.5	130
314	Promotion and inhibition effects of TiOx species on Rh inverse model catalysts. Applied Surface Science, 2014, 313, 432-439.	3.1	6
315	Three different clay-supported nanoscale zero-valent iron materials for industrial azo dye degradation: A comparative study. Journal of the Taiwan Institute of Chemical Engineers, 2014, 45, 2451-2461.	2.7	88
316	Metal loading determines the stabilization pathway for Co2+ in titanate nanowires: ion exchange vs. cluster formation. Physical Chemistry Chemical Physics, 2013, 15, 15917.	1.3	22
317	Effects of carbon nanotube functionalization on the agglomeration and sintering of supported Pd nanoparticles. Adsorption, 2013, 19, 501-508.	1.4	4
318	Self-assembling of 2,3-phenyl/thienyl-substituted acrylic acids over polycrystalline gold. Journal of Molecular Structure, 2013, 1044, 32-38.	1.8	3
319	Rh-Induced Support Transformation Phenomena in Titanate Nanowire and Nanotube Catalysts. Langmuir, 2013, 29, 3061-3072.	1.6	50
320	Radiation induced topotactic [2+2] dimerisation of acrylate derivatives among the layers of a CaFe layered double hydroxide followed by IR spectroscopy. Journal of Molecular Structure, 2013, 1044, 279-285.	1.8	4
321	Functionalized Low Defect Graphene Nanoribbons and Polyurethane Composite Film for Improved Gas Barrier and Mechanical Performances. ACS Nano, 2013, 7, 10380-10386.	7.3	124
322	Water Types and Their Relaxation Behavior in Partially Rehydrated CaFe-Mixed Binary Oxide Obtained from CaFe-Layered Double Hydroxide in the 155–298 K Temperature Range. Langmuir, 2013, 29, 13315-13321	. 1.6	16
323	Rehydration of dehydrated CaFe-L(ayered)D(ouble)H(ydroxide) followed by thermogravimetry, X-ray diffractometry and dielectric relaxation spectroscopy. Journal of Molecular Structure, 2013, 1044, 26-31.	1.8	11
324	Structural stability test of hexagonal CePO4 nanowires synthesized at ambient temperature. Journal of Molecular Structure, 2013, 1044, 94-98.	1.8	24

#	Article	IF	CITATIONS
325	Synthesis and characterization of WO3 nanowires and metal nanoparticle-WO3 nanowire composites. Journal of Molecular Structure, 2013, 1044, 99-103.	1.8	19
326	Structure and stability of pristine and Bi and/or Sb decorated titanate nanotubes. Journal of Molecular Structure, 2013, 1044, 104-108.	1.8	10
327	Luminescence properties of Ho3+ co-doped SrAl2O4:Eu2+, Dy3+ long-persistent phosphors synthesized with a solid-state method. Journal of Molecular Structure, 2013, 1044, 87-93.	1.8	12
328	Reconstruction of calcined MgAl- and NiMgAl-layered double hydroxides during glycerol dehydration and their recycling characteristics. Applied Clay Science, 2013, 80-81, 245-248.	2.6	27
329	Effect of planetary ball milling process parameters on the nitrogen adsorption properties of multiwall carbon nanotubes. Adsorption, 2013, 19, 687-694.	1.4	11
330	Studies on the thermal decomposition of multiwall carbon nanotubes under different atmospheres. Materials Letters, 2013, 90, 165-168.	1.3	138
331	The formation and stability of Rh nanostructures on TiO2(110) surface and TiOx encapsulation layers. Applied Surface Science, 2013, 280, 60-66.	3.1	9
332	Non-equilibrium transformation of titanate nanowires to nanotubes upon mechanochemical activation. RSC Advances, 2013, 3, 7681.	1.7	4
333	Molecular interactions between organic compounds and functionally modified multiwalled carbon nanotubes. Chemical Engineering Journal, 2013, 225, 144-152.	6.6	37
334	Room temperature hydrogen sensors based on metal decorated WO3 nanowires. Sensors and Actuators B: Chemical, 2013, 186, 90-95.	4.0	78
335	Interaction of Rh with Rh Nanoparticles Encapsulated by Ordered Ultrathin TiO1+x Film on TiO2(110) Surface. Langmuir, 2013, 29, 15868-15877.	1.6	9
336	Fine tuning the surface acidity of titanate nanostructures. Adsorption, 2013, 19, 695-700.	1.4	4
337	Zeolites. , 2013, , 819-858.		1
338	Carbon nanotubes synthesis over FeCo-based catalysts supported on SBA-16. Nanopages, 2013, 8, 1-8.	0.2	2
339	Nanoparticle Dispersions. , 2013, , 729-776.		5
340	Multi-Walled Carbon Nanotubes. , 2013, , 147-188.		37
341	Characterization of CNT Enhanced Conductive Adhesives in Terms of Thermal Conductivity. ECS Transactions, 2012, 44, 1011-1017.	0.3	2
342	A Possible Nanoreactor: CaFe-L(ayered)D(ouble)H(ydroxide) with Intercalated Cinnamate Derivatives. Materials Science Forum, 2012, 730-732, 65-70.	0.3	1

#	Article	IF	CITATIONS
343	Consequences of subacute intratracheal exposure of rats to cadmium oxide nanoparticles. Toxicology and Industrial Health, 2012, 28, 933-941.	0.6	18
344	Electrical resistivity and thermal properties of compatibilized multi-walled carbon nanotube/polypropylene composites. EXPRESS Polymer Letters, 2012, 6, 494-502.	1.1	38
345	Repeated simultaneous cortical electrophysiological and behavioral recording in rats exposed to manganese-containing nanoparticles. Acta Biologica Hungarica, 2012, 63, 426-440.	0.7	6
346	Microcystin-LR, a protein phosphatase inhibitor, induces alterations in mitotic chromatin and microtubule organization leading to the formation of micronuclei in Vicia faba. Annals of Botany, 2012, 110, 797-808.	1.4	19
347	Structural characterization of FeCo alloy nanoparticles embedded in SBA-16 and their catalytic application for carbon nanotubes production. RSC Advances, 2012, 2, 7886.	1.7	6
348	Comparison of Nanoscaled Palladium Catalysts Supported on Various Carbon Allotropes. Topics in Catalysis, 2012, 55, 865-872.	1.3	8
349	Preparation, Characterisation and Some Reactions of Organocatalysts Immobilised Between the Layers of a CaFe-Layered Double Hydroxide. Topics in Catalysis, 2012, 55, 858-864.	1.3	8
350	General and Electrophysiological Toxic Effects of Manganese in Rats following Subacute Administration in Dissolved and Nanoparticle Form. Scientific World Journal, The, 2012, 2012, 1-7.	0.8	12
351	Synthesis and Photocatalytic Performance of Titanium Dioxide Nanofibers and the Fabrication of Flexible Composite Films from Nanofibers. Journal of Nanoscience and Nanotechnology, 2012, 12, 1421-1424.	0.9	19
352	Synthesis and characterisation of coiled carbon nanotubes. Catalysis Today, 2012, 181, 33-39.	2.2	19
353	Nitrogen-Doped Anatase Nanofibers Decorated with Noble Metal Nanoparticles for Photocatalytic Production of Hydrogen. ACS Nano, 2011, 5, 5025-5030.	7.3	137
354	Layer-by-layer assembly of TiO ₂ nanowire/carbon nanotube films and characterization of their photocatalytic activity. Nanotechnology, 2011, 22, 195701.	1.3	23
355	Nervous system effects in rats on subacute exposure by lead-containing nanoparticles via the airways. Inhalation Toxicology, 2011, 23, 173-181.	0.8	45
356	Formation of CuPd and CuPt Bimetallic Nanotubes by Galvanic Replacement Reaction. Journal of Physical Chemistry C, 2011, 115, 9403-9409.	1.5	163
357	Optimization of the Catalytic Chemical Vapor Deposition Synthesis of Multiwall Carbon Nanotubes on FeCo(Ni)/SiO ₂ Aerogel Catalysts by Statistical Design of Experiments. Journal of Physical Chemistry C, 2011, 115, 5894-5902.	1.5	30
358	One-Step Preparation of FeCo Nanoparticles in a SBA-16 Matrix as Catalysts for Carbon Nanotubes Growth. Journal of Nanoscience and Nanotechnology, 2011, 11, 6735-6746.	0.9	6
359	Characterization of carbon thin films prepared by the thermal decomposition of spin coated polyacrylonitrile layers containing metal acetates. Thin Solid Films, 2011, 520, 57-63.	0.8	11
360	Mapping of Functionalized Regions on Carbon Nanotubes by Scanning Tunneling Microscopy. Journal of Physical Chemistry C, 2011, 115, 3229-3235.	1.5	10

#	Article	IF	CITATIONS
361	Synthesis and characterisation of alkaline earth-iron(III) double hydroxides. Chemical Papers, 2011, 65, .	1.0	10
362	A SEM, EDX and XAS characterization of Ba(II)Fe(III) layered double hydroxides. Journal of Molecular Structure, 2011, 993, 62-66.	1.8	11
363	Enhanced photocatalytic activity of TiO2 nanofibers and their flexible composite films: Decomposition of organic dyes and efficient H2 generation from ethanol-water mixtures. Nano Research, 2011, 4, 360-369.	5.8	109
364	Lowâ€ŧemperature growth of multiâ€walled carbon nanotubes by thermal CVD. Physica Status Solidi (B): Basic Research, 2011, 248, 2500-2503.	0.7	24
365	Thermal diffusivity of aligned multiâ€walled carbon nanotubes measured by the flash method. Physica Status Solidi (B): Basic Research, 2011, 248, 2508-2511.	0.7	12
366	Nervous system effects of dissolved and nanoparticulate cadmium in rats in subacute exposure. Journal of Applied Toxicology, 2011, 31, 471-476.	1.4	10
367	In situ synthesis of catalytic metal nanoparticle-PDMS membranes by thermal decomposition process. Composites Science and Technology, 2011, 71, 129-133.	3.8	22
368	Self-assembling of Z-α-pyridylcinnamic acid molecules over polycrystalline Ag and Au surfaces followed by FT-IR and atomic force microscopies. Journal of Molecular Structure, 2011, 993, 67-72.	1.8	0
369	Structure of the Au–Rh bimetallic system formed on titanate nanowires and nanotubes. Vacuum, 2011, 85, 1114-1119.	1.6	11
370	Probing the interaction of Au, Rh and bimetallic Au–Rh clusters with the TiO2 nanowire and nanotube support. Surface Science, 2011, 605, 1048-1055.	0.8	34
371	Compact USB measurement and analysis system for real-time fluctuation enhanced sensing. , 2011, , .		2
372	Somatic embryogenesis and regeneration from shoot primordia of Crocus heuffelianus. Plant Cell, Tissue and Organ Culture, 2010, 100, 349-353.	1.2	11
373	Moderate anisotropy in the electrical conductivity of bulk MWCNT/epoxy composites. Carbon, 2010, 48, 1918-1925.	5.4	29
374	Carbon nanotube based sensors and fluctuation enhanced sensing. Physica Status Solidi C: Current Topics in Solid State Physics, 2010, 7, 1217-1221.	0.8	6
375	INCREASING CHEMICAL SELECTIVITY OF CARBON NANOTUBE-BASED SENSORS BY FLUCTUATION-ENHANCED SENSING. Fluctuation and Noise Letters, 2010, 09, 277-287.	1.0	10
376	2-Magnon Raman Behavior of NiO Nanoparticles. , 2010, , .		2
377	Low-Temperature Large-Scale Synthesis and Electrical Testing of Ultralong Copper Nanowires. Langmuir, 2010, 26, 16496-16502.	1.6	149
378	Three-Dimensional Carbon Nanotube Scaffolds as Particulate Filters and Catalyst Support Membranes. ACS Nano, 2010, 4, 2003-2008.	7.3	72

#	Article	IF	CITATIONS
379	Functional neurotoxicity of Mn-containing nanoparticles in rats. Ecotoxicology and Environmental Safety, 2010, 73, 2004-2009.	2.9	54
380	Metal deposition and functional neurotoxicity in rats after 3–6 weeks nasal exposure by two physicochemical forms of manganese. Environmental Toxicology and Pharmacology, 2010, 30, 121-126.	2.0	14
381	Synthesis and properties of novel Ba(II)Fe(III) layered double hydroxides. Applied Clay Science, 2010, 48, 214-217.	2.6	25
382	Synthesis of Catalytic Porous Metallic Nanorods by Galvanic Exchange Reaction. Journal of Physical Chemistry C, 2010, 114, 389-393.	1.5	80
383	Laser-induced fluorescence measurements on CdSe quantum dots. Processing and Application of Ceramics, 2010, 4, 33-38.	0.4	14
384	Beneficial effect of multi-wall carbon nanotubes on the graphitization of polyacrylonitrile (PAN) coating. Processing and Application of Ceramics, 2010, 4, 59-62.	0.4	3
385	Numerical differentiation methods for the logarithmic derivative technique used in dielectric spectroscopy. Processing and Application of Ceramics, 2010, 4, 87-93.	0.4	1
386	Synthesis of Zinc Glycerolate Microstacks from a ZnO Nanorod Sacrificial Template. European Journal of Inorganic Chemistry, 2009, 2009, 3622-3627.	1.0	28
387	Synthesis and characterization of nickel catalysts supported on different carbon materials. Reaction Kinetics and Catalysis Letters, 2009, 96, 379-389.	0.6	14
388	A Novel Catalyst Type Containing Noble Metal Nanoparticles Supported on Mesoporous Carbon: Synthesis, Characterization and Catalytic Properties. Topics in Catalysis, 2009, 52, 1242-1250.	1.3	7
389	Adsorption of C6 hydrocarbon rings on mesoporous catalyst supports. Chemical Physics Letters, 2009, 482, 296-301.	1.2	4
390	Subacute intratracheal exposure of rats to manganese nanoparticles: Behavioral, electrophysiological, and general toxicological effects. Inhalation Toxicology, 2009, 21, 83-91.	0.8	31
391	Ionically Self-Assembled Polyelectrolyte-Based Carbon Nanotube Fibers. Chemistry of Materials, 2009, 21, 3062-3071.	3.2	32
392	Multiwall carbon nanotube films surfaceâ€doped with electroceramics for sensor applications. Physica Status Solidi (B): Basic Research, 2008, 245, 2331-2334.	0.7	12
393	Inkjet printed resistive and chemicalâ€FET carbon nanotube gas sensors. Physica Status Solidi (B): Basic Research, 2008, 245, 2335-2338.	0.7	23
394	Drift effect of fluctuation enhanced gas sensing on carbon nanotube sensors. Physica Status Solidi (B): Basic Research, 2008, 245, 2343-2346.	0.7	6
395	Fluctuation enhanced gas sensing on functionalized carbon nanotube thin films. Physica Status Solidi (B): Basic Research, 2008, 245, 2339-2342.	0.7	9
396	Fine tuning the coverage of a titanate nanowire layer on a glass substrate. Chemical Physics Letters, 2008, 460, 191-195.	1.2	7

#	Article	IF	CITATIONS
397	Pyroelectric temperature sensitization of multi-wall carbon nanotube papers. Carbon, 2008, 46, 1262-1265.	5.4	6
398	Sonochemical Synthesis of Inorganic Nanoparticles. NATO Science for Peace and Security Series B: Physics and Biophysics, 2008, , 369-372.	0.2	9
399	Degradation of pure and waste polyolefins and PVC in the presence of modified porous catalysts. Studies in Surface Science and Catalysis, 2008, , 1021-1026.	1.5	3
400	Improving the performance of functionalized carbon nanotube thin film sensors by fluctuation enhanced sensing. , 2008, , .		1
401	Functionalization of Multi-Walled Carbon Nanotubes (MWCNTS). NATO Science for Peace and Security Series B: Physics and Biophysics, 2008, , 365-368.	0.2	4
402	Carbon Nanotubes as Ceramic Matrix Reinforcements. Materials Science Forum, 2007, 537-538, 97-104.	0.3	1
403	Silicon Nitride – Carbon Nanotube Composites. Materials Science Forum, 2007, 554, 123-128.	0.3	2
404	Hydrothermal Conversion of Self-Assembled Titanate Nanotubes into Nanowires in a Revolving Autoclave. Chemistry of Materials, 2007, 19, 927-931.	3.2	154
405	Chemical functionalisation of titania nanotubes and their utilisation for the fabrication of reinforced polystyrene composites. Journal of Materials Chemistry, 2007, 17, 2351.	6.7	69
406	Structure and gas permeability of multi-wall carbon nanotube buckypapers. Carbon, 2007, 45, 1176-1184.	5.4	152
407	Controlling the pore diameter distribution of multi-wall carbon nanotube buckypapers. Carbon, 2007, 45, 1696-1698.	5.4	71
408	Spectroscopic studies on self-supporting multi-wall carbon nanotube based composite films for sensor applications. Journal of Molecular Structure, 2007, 834-836, 471-476.	1.8	16
409	Spectroscopic studies on the formation kinetics of SnO2 nanoparticles synthesized in a planetary ball mill. Journal of Molecular Structure, 2007, 834-836, 430-434.	1.8	17
410	Pre-prepared platinum nanoparticles supported on SBA-15 – preparation, pretreatment conditions and catalytic properties. Catalysis Letters, 2007, 113, 19-28.	1.4	27
411	Morphology and N2 Permeability of Multi-Wall Carbon Nanotube—Teflon Membranes. Journal of Nanoscience and Nanotechnology, 2007, 7, 1604-1610.	0.9	7
412	Processing, mechanical and thermophysical properties of silicon nitride based composites with carbon nanotubes and graphene. Processing and Application of Ceramics, 2007, 1, 35-41.	0.4	4
413	Carbon Nanotubes - Towards Artificial Nose Implementation. , 2006, , .		0
414	Multiwall carbon nanotube modified vinylester and vinylester – based hybrid resins. Composites Part A: Applied Science and Manufacturing, 2006, 37, 1252-1259.	3.8	78

#	Article	IF	CITATIONS
415	Synthesis, characterization and use of coiled carbon nanotubes. Nanopages, 2006, 1, 263-293.	0.2	6
416	Synthesis of Multiwall Carbon Nanotubes in the Pore System and/or on the Outer Surface of Mesoporous MCM-41 Structures of Various Morphology. Nanopages, 2006, 1, 97-117.	0.2	1
417	Application of carbon nanotubes to silicon nitride matrix reinforcements. Current Applied Physics, 2006, 6, 124-130.	1.1	49
418	Tubular inorganic nanostructures. Current Applied Physics, 2006, 6, 212-215.	1.1	8
419	Development of CNT/Si3N4 composites with improved mechanical and electrical properties. Composites Part B: Engineering, 2006, 37, 418-424.	5.9	104
420	Functionalization of carbon nanotubes with oligonucleotide in solutions — Production of nanotube chips. Journal of Molecular Liquids, 2006, 129, 33-38.	2.3	0
421	CO hydrogenation over cobalt and iron catalysts supported over multiwall carbon nanotubes: Effect of preparation. Journal of Catalysis, 2006, 244, 24-32.	3.1	101
422	Isomorphous Substitution in Zeolites. , 2006, , 365-478.		9
423	Development of CNT-Silicon Nitrides with Improved Mechanical and Electrical Properties. Advances in Science and Technology, 2006, 45, 1723-1728.	0.2	6
424	CARBON NANOTUBES AS CERAMIC MATRIX REINFORCEMENTS. , 2006, , 221-222.		4
425	IR spectroscopic investigation of the particle size and morphology of platinum nanoparticles supported on mesoporous silicate. Studies in Surface Science and Catalysis, 2005, 158, 1351-1358.	1.5	2
426	Morphological characterization of mesoporous silicate–carbon nanocomposites. Microporous and Mesoporous Materials, 2005, 80, 85-94.	2.2	9
427	IR and NMR spectroscopic characterization of graphitization process occurring in the pores of mesoporous silicates in formation of carbon nanotubes. Journal of Molecular Structure, 2005, 744-747, 93-99.	1.8	4
428	Long-time low-impact ball milling of multi-wall carbon nanotubes. Carbon, 2005, 43, 994-1000.	5.4	138
429	Processing of carbon nanotube reinforced silicon nitride composites by spark plasma sintering. Composites Science and Technology, 2005, 65, 727-733.	3.8	101
430	Complex-assisted one-step synthesis of ion-exchangeable titanate nanotubes decorated with CdS nanoparticles. Chemical Physics Letters, 2005, 411, 445-449.	1.2	70
431	Highly perfect inner tubes in CVD grown double-wall carbon nanotubes. Chemical Physics Letters, 2005, 413, 506-511.	1.2	13
432	Thermal behavior of multiwall carbon nanotube/zeolite nanocomposites. Journal of Thermal Analysis and Calorimetry, 2005, 79, 567-572.	2.0	10

#	Article	IF	CITATIONS
433	Thermal stability of platinum particles embedded in mesoporous silicates. Journal of Thermal Analysis and Calorimetry, 2005, 79, 573-577.	2.0	8
434	Infrared spectroscopy studies of cyclohexene hydrogenation and dehydrogenation catalyzed by platinum nanoparticles supported on mesoporous silicate (SBA-15). Part 1: The role of particle size of Pt nanocrystals supported on SBA-15 silicate. Catalysis Letters, 2005, 101, 159-167.	1.4	13
435	Development of Preparation Processes for CNT/Si ₃ N ₄ Composites. Key Engineering Materials, 2005, 290, 135-141.	0.4	5
436	Vibrational Spectroscopic Studies on the Formation of Ion-exchangeable Titania Nanotubes. AIP Conference Proceedings, 2005, , .	0.3	1
437	Mechanical Degradation of Carbon Nanotubes: ESR Investigations. Materials Research Society Symposia Proceedings, 2005, 887, 1.	0.1	0
438	Continuous Production of Polycarbonate-Carbon Nanotube Composites. Journal of Polymer Engineering, 2005, 25, .	0.6	1
439	Carbon Nanotubes – on the Eve of Success?. Materials Science Forum, 2005, 473-474, 141-146.	0.3	1
440	Oriented Crystal Growth Model Explains the Formation of Titania Nanotubes. Journal of Physical Chemistry B, 2005, 109, 17781-17783.	1.2	159
441	Hydrodechlorination of carbon tetrachloride on Pt-containing zeolites. Studies in Surface Science and Catalysis, 2004, 154, 2536-2542.	1.5	2
442	Synthesis and characterization of spherical mesoporous MCM-41 materials containing transition metals. Studies in Surface Science and Catalysis, 2004, , 813-819.	1.5	1
443	On the Growth Mechanism of Single-Walled Carbon Nanotubes by Catalytic Carbon Vapor Deposition on Supported Metal Catalysts. Journal of Nanoscience and Nanotechnology, 2004, 4, 326-345.	0.9	45
444	Production of multiwall carbon nanotubes in the modified pore system of mesoporous silicates. Diamond and Related Materials, 2004, 13, 1322-1326.	1.8	5
445	Determination of traces of elemental impurities in single walled (SWNT) and multi walled (MWNT) pristine and purified carbon nanotubes by instrumental neutron activation analysis. Journal of Radioanalytical and Nuclear Chemistry, 2004, 262, 31-34.	0.7	12
446	Spherical mesoporous MCM-41 materials containing transition metals: synthesis and characterization. Applied Catalysis A: General, 2004, 272, 257-266.	2.2	102
447	End morphology of ball milled carbon nanotubes. Carbon, 2004, 42, 2001-2008.	5.4	83
448	Photosensitization of ion-exchangeable titanate nanotubes by CdS nanoparticles. Chemical Physics Letters, 2004, 399, 512-515.	1.2	175
449	XPS study of multiwall carbon nanotube synthesis on Ni-, V-, and Ni, V-ZSM-5 catalysts. Applied Catalysis A: General, 2004, 260, 55-61.	2.2	44
450	The dynamics of H2 and N2 sorption in carbon nanotubes. Applied Surface Science, 2004, 238, 73-76.	3.1	4

#	Article	IF	CITATIONS
451	Synthesis of carbon nanotubes with tailor made diameter in the channels of micelle-templated silicas. Studies in Surface Science and Catalysis, 2004, , 911-916.	1.5	0
452	Quantitative Characterization of Hydrophilicâ^'Hydrophobic Properties of MWNTs Surfaces. Langmuir, 2004, 20, 1656-1661.	1.6	44
453	Comparison of Fe/Al <tex>\$_2\$</tex> O <tex>\$_3\$</tex> and Fe, Co/Al <tex>\$_2\$</tex> O <tex>\$_3\$</tex> Catalysts Used for Production of Carbon Nanotubes From Acetylene by CCVD. IEEE Nanotechnology Magazine, 2004, 3, 73-79.	1.1	19
454	Synthetic Insertion of Gold Nanoparticles into Mesoporous Silica. Chemistry of Materials, 2003, 15, 1242-1248.	3.2	175
455	STM investigation of carbon nanotubes connected by functional groups. Materials Science and Engineering C, 2003, 23, 1007-1011.	3.8	31
456	On the role of catalyst, catalyst support and their interaction in synthesis of carbon nanotubes by CCVD. Materials Chemistry and Physics, 2003, 77, 536-541.	2.0	69
457	Synthesis Insertion of Gold Nanoparticles into Mesoporous Silica ChemInform, 2003, 34, no.	0.1	0
458	Sonication assisted gold deposition on multiwall carbon nanotubes. Chemical Physics Letters, 2003, 372, 848-852.	1.2	33
459	Preparation and characterization of carbon nanotube reinforced silicon nitride composites. Materials Science and Engineering C, 2003, 23, 1133-1137.	3.8	176
460	IR spectroscopic reinvestigation of the generation of acid sites in Pt-containing faujasite zeolites. Journal of Molecular Structure, 2003, 651-653, 191-197.	1.8	16
461	Structural consequences of mild oxidative template removal in the synthesis of modified MCM-41 silicates. Journal of Molecular Structure, 2003, 651-653, 323-330.	1.8	10
462	Intercalating amino acid guests into montmorillonite host. Journal of Molecular Structure, 2003, 651-653, 335-340.	1.8	61
463	Synthesis and characterization of hyperbranched mesoporous silica SBA-15. Chemical Communications, 2003, , 314.	2.2	26
464	Encapsulation of Metal (Au, Ag, Pt) Nanoparticles into the Mesoporous SBA-15 Structure. Langmuir, 2003, 19, 4396-4401.	1.6	163
465	Binary solvent mixture adsorption as a characterisation tool to determine the hydrophilic/hydrophobic properties of multiwall carbon nanotubes. Chemical Communications, 2003, , 2746.	2.2	5
466	"Wash and goâ€ŧ sodium chloride as an easily removable catalyst support for the synthesis of carbon nanotubes. PhysChemComm, 2003, 6, 40-41.	0.8	15
467	Geometrical Effects of Wave Functions of Carbon Nanosystems. AIP Conference Proceedings, 2003, , .	0.3	1
468	Synthesis Procedures for Production of Carbon Nanotube Junctions. AIP Conference Proceedings, 2003, , .	0.3	6

#	Article	IF	CITATIONS
469	Comparison of Fe/Al 2 O 3 and Fe,Co/Al 2 O 3 catalysts used for production of carbon nanotubes from acetylene by CCVD. , 2003, , .		3
470	STM investigation of carbon nanotubes completely covered with functional groups. , 2003, , .		0
471	Synthesis procedures for production of carbon nanotube junctions. , 2003, , .		4
472	Mesoporous Silicates as Nanoreactors for Carbon Nanotube Production in the Absence of Transition Metal Catalysts. Journal of Nanoscience and Nanotechnology, 2003, 3, 111-119.	0.9	8
473	Mechanisms of Controlled Growth Of Metallic Nanocrystals. Materials Research Society Symposia Proceedings, 2002, 721, 1.	0.1	0
474	Hydrodechlorination of chlorinated compounds on different zeolites. Studies in Surface Science and Catalysis, 2002, 142, 927-934.	1.5	5
475	Interconnecting Carbon Nanotubes with an Inorganic Metal Complex. Journal of the American Chemical Society, 2002, 124, 13694-13695.	6.6	116
476	Mechano-chemical functionalization of carbon nanotubes. AIP Conference Proceedings, 2002, , .	0.3	2
477	Nanocrystal Templating of Silica Mesopores with Tunable Pore Sizes. Nano Letters, 2002, 2, 907-910.	4.5	84
478	Mesoporous silicates as nanoreactors for synthesis of carbon nanotubes. PhysChemComm, 2002, 5, 138-141.	0.8	2
479	The role of zeotype catalyst support in the synthesis of carbon nanotubes by CCVD. Studies in Surface Science and Catalysis, 2002, , 541-548.	1.5	2
480	Comparative Study of Catalysts containing Transition Metals in Production of Carbon Nanotubes. AIP Conference Proceedings, 2002, , .	0.3	0
481	Full three-dimensional wave-packet dynamical calculations of STM images of nanotube Y-junctions. AIP Conference Proceedings, 2002, , .	0.3	1
482	Modification of multiwalled carbon nanotubes by different breaking processes. European Physical Journal Special Topics, 2002, 12, 107-112.	0.2	2
483	Mechanical cut of carbon nanotubes. AIP Conference Proceedings, 2002, , .	0.3	0
484	Mechanical and chemical breaking of multiwalled carbon nanotubes. Catalysis Today, 2002, 76, 3-10.	2.2	47
485	Alumina and silica supported metal catalysts for the production of carbon nanotubes. Journal of Molecular Catalysis A, 2002, 181, 57-62.	4.8	132
486	Synthesis, characterisation and catalytic applications of sol–gel derived silica–phosphotungstic acid composites. Applied Catalysis A: General, 2002, 228, 83-94.	2.2	76

#	Article	IF	CITATIONS
487	Heterogeneous catalytic production and mechanical resistance of nanotubes prepared on magnesium oxide supported Co-based catalysts. Applied Catalysis A: General, 2002, 229, 229-233.	2.2	26
488	Flexibility of the MCM-41 structure: pore expansion and wall-thickening in MCM-41 derivatives. Applied Catalysis A: General, 2002, 232, 67-76.	2.2	7
489	Catalyst traces and other impurities in chemically purified carbon nanotubes grown by CVD. Materials Science and Engineering C, 2002, 19, 9-13.	3.8	45
490	Production of carbon nanotubes inside the pores of mesoporous silicates. Chemical Physics Letters, 2002, 359, 95-100.	1.2	36
491	Large scale production of short functionalized carbon nanotubes. Chemical Physics Letters, 2002, 360, 429-435.	1.2	176
492	Title is missing!. Catalysis Letters, 2002, 81, 137-140.	1.4	76
493	Multinuclear Magnetic Resonance Characterization of Solid Catalysts and Their Reactions in the Adsorbed State. , 2002, , 219-229.		1
494	Hydrogen storage in carbon nanotubes produced by CVD. European Physical Journal Special Topics, 2002, 12, 129-137.	0.2	2
495	Alumina and Zeolites as Catalysts for Decomposition and Transformation of Chlorofluorocarbons Studied by Multinuclear NMR Methods. , 2002, , 559-564.		0
496	Surface Fractal Properties of Morphologically Different Solâ^'Gel Derived Silicates. Chemistry of Materials, 2001, 13, 345-349.	3.2	12
497	XPS characterisation of catalysts during production of multiwalled carbon nanotubes. Physical Chemistry Chemical Physics, 2001, 3, 155-158.	1.3	48
498	Catalyst traces after chemical purification in CVD grown carbon nanotubes. AIP Conference Proceedings, 2001, , .	0.3	1
499	Functional groups generated by mechanical and chemical breaking of multiwall carbon nanotubes. AIP Conference Proceedings, 2001, , .	0.3	3
500	Large scale synthesis of carbon nanotubes and their composite materials. AIP Conference Proceedings, 2001, , .	0.3	1
501	Gram scale production of singlewall carbon nanotubes by catalytic decomposition of hydrocarbons. AIP Conference Proceedings, 2001, , .	0.3	1
502	Structure comparison of nanotubes produced by different processes. Applied Physics A: Materials Science and Processing, 2001, 72, S185-S188.	1.1	3
503	UV–VIS investigations on Co, Fe and Ni incorporated into sol–gel SiO2–TiO2 matrices. Journal of Molecular Structure, 2001, 563-564, 403-407.	1.8	23
504	An FT-IR and UV–VIS study on the structure and acidity of sol–gel derived silica foams. Journal of Molecular Structure, 2001, 563-564, 409-412.	1.8	15

#	Article	IF	CITATIONS
505	Intercalation of various oxide species in-between Laponite layers studied by spectroscopic methods. Journal of Molecular Structure, 2001, 563-564, 417-420.	1.8	6
506	IR investigation of the transformation of propyne to propadiene on solid surfaces. Journal of Molecular Structure, 2001, 565-566, 115-120.	1.8	2
507	Spectroscopy in environmental protection, comparative IR and 13C NMR study of chlorofluorocarbons. Journal of Molecular Structure, 2001, 563-564, 167-171.	1.8	1
508	IR spectroscopic studies on the surface chemistry of mordenites modified by ceria. Journal of Molecular Structure, 2001, 563-564, 413-416.	1.8	2
509	Infrared spectroscopic study of benzene and chlorobenzene adsorption on Pt,Cu- and Pt, CoZSM-5 bimetallic zeolite catalysts. Journal of Molecular Structure, 2001, 563-564, 435-438.	1.8	4
510	An FT-IR study on Diels–Alder reactions catalysed by heteropoly acid containing sol–gel silica. Journal of Molecular Structure, 2001, 565-566, 121-124.	1.8	2
511	Production of short carbon nanotubes with open tips by ball milling. Chemical Physics Letters, 2001, 335, 1-8.	1.2	272
512	The Acidity and Catalytic Activity of Supported Acidic Cesium Dodecatungstophosphates Studied by MAS NMR, FTIR, and Catalytic Test Reactions. Journal of Catalysis, 2001, 202, 379-386.	3.1	30
513	Production of Carbon Nanotubes on Different Metal Supported Catalysts. Reaction Kinetics and Catalysis Letters, 2001, 74, 329-336.	0.6	16
514	Title is missing!. Reaction Kinetics and Catalysis Letters, 2001, 74, 363-370.	0.6	1
515	Transformation of Chlorofluorocarbons on Zeolites: Dealumination. Reaction Kinetics and Catalysis Letters, 2001, 74, 309-316.	0.6	2
516	29-P-18-Preparation using ozone treatment, characteration and application of isomorphously substituted Ti, V- and Zr-MCM-41 catalysts. Studies in Surface Science and Catalysis, 2001, , 315.	1.5	0
517	Catalytic Production, Purification, Characterization and Application of Single-and Multiwall Carbon Nanotubes. , 2001, , 85-109.		7
518	IR spectroscopic investigations of the adsorption of benzoyl chloride in zeolites. Vibrational Spectroscopy, 2000, 22, 29-37.	1.2	6
519	Preparation, characterization and application of the magadiite based mesoporous composite material of catalytic interest. Microporous and Mesoporous Materials, 2000, 35-36, 631-641.	2.2	18
520	The advantages of ozone treatment in the preparation of tubular silica structures. Applied Catalysis A: General, 2000, 203, L1-L4.	2.2	19
521	Control of the outer diameter of thin carbon nanotubes synthesized by catalytic decomposition of hydrocarbons. Chemical Physics Letters, 2000, 317, 71-76.	1.2	164
522	Large-scale synthesis of single-wall carbon nanotubes by catalytic chemical vapor deposition (CCVD) method. Chemical Physics Letters, 2000, 317, 83-89.	1.2	427

#	Article	IF	CITATIONS
523	Observation of site selective binding in a polymer nanotube composite. Journal of Materials Science Letters, 2000, 19, 2239-2241.	0.5	59
524	Synthesis, characterization and catalytic application of inorganic nanotubes. Studies in Surface Science and Catalysis, 2000, , 1115-1120.	1.5	2
525	Nanostructured carbon generated by chemical vapor deposition from acetylene on surfaces pretreated by a combination of physical and chemical methods. Journal of Materials Research, 2000, 15, 2087-2090.	1.2	3
526	Selective nucleation and growth of carbon nanotubes at the CoSi2/Si interface. Applied Physics Letters, 2000, 76, 706-708.	1.5	9
527	Transformation of chlorinated compounds on different zeolites under oxidative and reductive conditions. Studies in Surface Science and Catalysis, 2000, 130, 1235-1240.	1.5	8
528	Production of differently shaped multi-wall carbon nanotubes using various cobalt supported catalysts. Physical Chemistry Chemical Physics, 2000, 2, 163-170.	1.3	57
529	Catalytic synthesis of carbon nanotubes over Co, Fe and Ni containing conventional and sol–gel silica–aluminas. Physical Chemistry Chemical Physics, 2000, 2, 3071-3076.	1.3	114
530	Multinuclear MAS NMR investigation of zeolites reacted with chlorofluorocarbons. Journal of Molecular Structure, 1999, 482-483, 359-364.	1.8	9
531	Acidity of bimetallic silica composites prepared by a complexing agent assisted sol–gel method. Journal of Molecular Structure, 1999, 482-483, 39-42.	1.8	2
532	Infrared spectroscopic studies on the surface chemistry of bimetallic zeolite systems. Acidity of Pt,Co- and Pt,CuZSM-5 zeolites. Journal of Molecular Structure, 1999, 482-483, 1-5.	1.8	9
533	In situ MAS 13C-NMR studies of surface intermediates formed upon interaction of CCl2F2 (CFC-12) with NaY-FAU and HZSM-5-MFI zeolites. Colloids and Surfaces A: Physicochemical and Engineering Aspects, 1999, 158, 35-42.	2.3	6
534	Bulk production of quasi-aligned carbon nanotube bundles by the catalytic chemical vapour deposition (CCVD) method. Chemical Physics Letters, 1999, 303, 117-124.	1.2	165
535	Spectroscopic investigations of the decomposition of CCl2F2 on three different types of zeolites. Studies in Surface Science and Catalysis, 1999, 125, 245-252.	1.5	13
536	Synthesis of single-wall carbon nanotubesby catalytic decomposition of hydrocarbons. Chemical Communications, 1999, , 1343-1344.	2.2	107
537	Metal mixtures catalysed carbon nanotube synthesis. , 1999, , .		0
538	Solid state MAS NMR investigation of Y-type zeolites reacted with chlorofluorocarbons. Applied Catalysis B: Environmental, 1998, 17, 157-166.	10.8	36
539	Zeolites in the environmental protection $\hat{a} \in$ " Decomposition of chlorofluorocarbons over zeolite catalysts. Studies in Surface Science and Catalysis, 1997, , 1509-1516.	1.5	11
540	Influence of pretreatment conditions on acidity of cobalt-based bimetallic systems in NaY zeolite. Catalysis Letters, 1997, 44, 7-10.	1.4	18

#	Article	IF	CITATIONS
541	Spectroscopic behavior in the adsorption of COî—,Cl2 mixtures on NaY-FAU zeolite. Vibrational Spectroscopy, 1997, 15, 37-42.	1.2	5
542	Fermi resonance of C1 chlorine compounds in the adsorbed phase of zeolites. An FTIR and MAS NMR spectroscopic study. Journal of Molecular Structure, 1997, 410-411, 89-93.	1.8	0
543	FT-IR Spectroscopic Investigation of the Transformation of Allyl Cyanide in the Presence of Butyl-lithium. , 1997, , 203-205.		0
544	Infrared spectroscopic study of adsorption and reactions of methyl chloride on acidic, neutral and basic zeolites. Applied Catalysis B: Environmental, 1996, 8, 391-404.	10.8	32
545	Suggested binding mechanism of the HIV-gp120 to its CD4 receptor. Computational and Theoretical Chemistry, 1996, 367, 159-186.	1.5	6
546	Indium and gallium containing ZSM-5 zeolites: acidity and catalytic activity in propane transformation. Catalysis Today, 1996, 31, 293-304.	2.2	51
547	Interconversion of unsaturated C4 nitriles under basic conditions II. Catalytic and FTIR study over basic zeolites. Applied Catalysis A: General, 1996, 146, 331-338.	2.2	4
548	Interconversion of unsaturated C4 nitriles under basic conditions I. An IR-UV—VIS spectroscopic study in the presence of butyllithium. Applied Catalysis A: General, 1996, 146, 323-330.	2.2	6
549	Conformational Mapping of Amyloid Peptides from the Putative Neurotoxic 25-35 Region. Biochemical and Biophysical Research Communications, 1994, 205, 120-126.	1.0	24
550	Preparation of Si ₃ N ₄ Composites with Single Wall Carbon Nanotube and Exfoliated Graphite. Materials Science Forum, 0, 589, 409-414.	0.3	2
551	Electronic work function modulation of phosphorene by thermal oxidation. 2D Materials, 0, , .	2.0	3
552	Rapid direct cathodic voltammetric determination of insecticide flonicamid by renewable silver-amalgam film electrode. International Journal of Environmental Analytical Chemistry, 0, , 1-15.	1.8	0
553	Functionalized Mesoporous Silica Nanoparticles for Drug-Delivery to Multidrug-Resistant Cancer Cells. International Journal of Nanomedicine, 0, Volume 17, 3079-3096.	3.3	6